Manuscript Details

Manuscript number	MEATSCI_2019_1106
Title	Use of Non-destructive Techniques for the Quality Evaluation of Fresh Meat: A Review
Article type	Invited review article

Abstract

The development of non-destructive methodology based on Near-Infrared Reflectance spectroscopy (NIRs), Hyperspectral Imaging (HSI), Nuclear Magnetic Resonance (NMR) and Magnetic Resonance Imaging (MRI) techniques to determine quality characteristics of fresh meat has been reviewed in this study, which has been mainly focused on researches published in the last decade. This review has put special attention on the instrumentation, data acquisition and main applications of each technique, finding a wide variety of possibilities of systems and methodologies as well as evidences of accurate and promising results. Most analysed samples have been pork and beef, followed by lamb and chicken, while there are few studies on fresh meat from rabbit and duck. The evaluation of the methodology exposed in the revised articles has been carried out in an experimental way but lacking real application in the meat industry. For that, these non-destructive techniques should be improved, especially regarding the speed, price and influence of external factors.

Keywords	Near-Infrared Reflectance spectroscopy; Hyperspectral Imaging; Nuclear Magnetic Resonance; Magnetic Resonance Imaging; fresh meat; non-destructive analysis.
Taxonomy	Meat, Analytical Method

Corresponding Author	Trinidad Perez-Palacios
Corresponding Author's Institution	University of Extremadura
Order of Authors	Teresa Antequera, Daniel Caballero, Silvia Grassi, Bethany Uttaro, Trinidad Perez-Palacios

Suggested reviewers	Xinglian Xu, Kate Kemsley, Yael Vodovotz, Da-Wen Sun

Submission Files Included in this PDF

File Name [File Type]

cover letter.docx [Cover Letter]

review non destructive methods 13 12 19_BU.docx [Manuscript File]

Figure 1 NIRs.docx [Figure]

Figure 2.docx [Figure]

Figure 3 NMR.docx [Figure]

Figure 4 MRI hams.docx [Figure]

Table 1 NIRs 13 12 19.docx [Table]

Table 2 HSI 13 12 19.docx [Table]

Table 3 NMR 13 12 19.docx [Table]

Table 4 MRI 13 12 19.docx [Table]

declaration-of-competing-interests signed.pdf [Conflict of Interest]

author contribution.docx [Author Statement]

To view all the submission files, including those not included in the PDF, click on the manuscript title on your EVISE Homepage, then click 'Download zip file'.

Trinidad Pérez Palacios
Research Institute of Meat and Meat Product
University of Extremadura

Cáceres, december 2019

Dear editor,

Please find enclosed the second revised version of the manuscript entitled “Use of Non-destructive Techniques for the Quality Evaluation of Fresh Meat: A Review” to be considered for publishing in *Meat Science.*

The present manuscript is a review aimed on published studies about the use of NIRs, HSI, NMR and MRI to determine the quality of fresh meat, paying special attention to the methodologies used (instrumentation, data acquisition and data analysis) and their applications.

We confirm that this work is original and has not been published elsewhere nor it is currently under consideration for publication elsewhere. We state that there are no known conflicts of interest associated with this publication. We declare that the manuscript is prepared strictly according to the Journal format as provided in the instruction to authors.

Please address all correspondence concerning this manuscript to me at triny@unex.es.

Thank you for your consideration of this manuscript.

Yours sincerely,

Trinidad Pérez Palacios
Research Institute of Meat and Meat Product
University of Extremadura
10003-Cáceres
Spain

TITLE

Use of Non-destructive Techniques for the Quality Evaluation of Fresh Meat: A Review

AUTHORS AND AFFILIATIONS

Teresa Antequera [1], Daniel Caballero [1,2τ], Silvia Grassi [3], Bethany Uttaro [4], Trinidad Perez-Palacios [1,*].

[1] Food Technology Department, Meat and Meat Products Research Institute, University of Extremadura, Av. Ciencias S/N, ES-10003, Cáceres, Spain.

[2] Chemometrics and Analytical Technology Section, Food Technology Department, Faculty of Science, University of Copenhagen, Rolighedsvej 26, DK-1958, Frederiksberg C, Denmark. [τ] Present address.

[3] Department of Food, Environmental and Nutritional Sciences, Università degli Studi di Milano, Via Mangiagalli 25, IT-20133, Milano, Italy.

[4] Lacombe Research and Development Centre, Agriculture & Agri-Food Canada, 6000 C and E Trail, Lacombe, Alberta, Canada, T4L 1W1.

*CORRESPONDING AUTHOR
Trinidad Pérez Palacios
e-mail address: triny@unex.es
Telephone: +34927251052 Ext. 51052
Fax: +34927257110

'Declarations of interest: none'

ABSTRACT

The development of non-destructive methodology based on Near-Infrared Reflectance spectroscopy (NIRs), Hyperspectral Imaging (HSI), Nuclear Magnetic Resonance (NMR) and Magnetic Resonance Imaging (MRI) techniques to determine quality characteristics of fresh meat has been reviewed in this study, which has been mainly focused on researches published in the last decade.

This review has put special attention on the instrumentation, data acquisition and main applications of each technique, finding a wide variety of possibilities of systems and methodologies as well as evidences of accurate and promising results. Most analysed samples have been pork and beef, followed by lamb and chicken, while there are few studies on fresh meat from rabbit and duck.

The evaluation of the methodology exposed in the revised articles has been carried out in an experimental way but lacking real application in the meat industry. For that, these non-destructive techniques should be improved, especially regarding the speed, price and influence of external factors.

KEY WORDS

Near-Infrared Reflectance spectroscopy; Hyperspectral Imaging; Nuclear Magnetic Resonance; Magnetic Resonance Imaging; fresh meat; non-destructive analysis.

1. INTRODUCTION

Meat and meat products are high appreciated, which is principally due to their sensory properties, but their nutritional composition is also relevant. Evaluation of meat and meat products by means of many physico-chemical, sensory and microbiological analysis is the subject of the industry, laboratories and researches, in order to i) guarantee the global quality of these kind of food, ii) assure that they accomplish the legal requirements and iii) give response to the demands of the consumers.

Physico-chemical characteristics, such as pH, colour, water activity, content of moisture, lipids, protein or salt, and sensory attributes are the most demanded parameters to be determined. However, traditional methodology applied to carry out these analyses require the destruction of the meat pieces to correctly take a representative sample. These techniques also consume solvents, take long times and are tedious. Besides, a trained panel is needed to evaluate the samples in the case of the sensory analysis (Pérez-Palacios, Caballero, Caro, Rodríguez, & Antequera, 2014).

As response to these drawbacks, several studies have been developed to evaluate the capability of different techniques based on images and/or spectra to analyse quality parameters of meat and meat products in a non-destructive way, with the final aim of proposing the evaluated techniques as alternative and/or complementary to the traditional methods. Couple-Charges Devices cameras (Cameras CCD), computed tomography (CT), Near-Infrared Reflectance spectroscopy (NIRs), Hyperspectral Imaging (HSI), Nuclear Magnetic Resonance (NMR) and the Magnetic Resonance Imaging (MRI) are some of these proposed techniques.

The present manuscript was focused on reviewing the published studies at evaluating the use of NIRs, HSI, NMR and MRI to determine the quality of fresh meat, paying special attention to the methodologies used (instrumentation, data acquisition and data analysis) and their applications.

Thus, this review article has been organized as follow: section 2 exposes the scientific searches that have been carried out; section 3 is about the instrumentation of each of the focused technologies; section 4 deals with the procedure for the data acquisition and methods for the data analysis; section 5 presents the latest applications of NIRs, HSI, NMR and MRI techniques for the analysis of fresh meat; section 6 discusses the advantages and disadvantages of these non-destructive methodologies; and section 7 summarizes conclusions for each technology and points out some future goals.

2. SCIENTIFIC SEARCHES

The searches on the scientific literature were carried out by using *Scopus*, *Science Direct* and *Web of Science*. The key words used were “meat” in combination to “Near Infrared Reflectance spectroscopy” or “NIR” or “NIRs” or “Hyperspectral Imaging” or “HSI” or “Nuclear Magnetic

Resonance" or "NMR" or "Magnetic Resonance Imaging" or "Magnetic Resonance Images" or "MRI", and the areas of interest were limited to Food Science and Technology and Science Technology Other Topics. In this way, around 140, 200, 170 and 150 documents were retained for NIRs, HSI, NMR and MRI, respectively. Then, only the publications that fulfilled the research aim (research papers at evaluating the use of NIRs, HSI, NMR, or MRI to analyse fresh meat) in approximately the last ten years were selected (25 + 31 + 9 + 10 documents, respectively) to be exhaustively analysed.

3. INSTRUMENTATION

3.1. NIRs

The NIRs method works in the region of the electromagnetic spectra from approximately 780 nm to 2500 nm, although quite often VIS wavelengths (~400-700 nm) are also collected. Generally speaking, there are three formats of NIRs equipment – benchtop, portable, and miniature, all of which are being used in fresh meat research. Benchtop equipment, such as the FOSS family of analysers, may be operated under controlled environmental conditions (temperature, humidity, airflow) and are often used in laboratory situations, usually with ground meat. Portable equipment such as the ASD range of spectrometers may or may not be more compact, but are more tolerant to environmental operating conditions, and are often used on intact meat. With the advent of microelectromechanical systems (MEMS) and micro-optical electromechanical systems (MOEMS), the numbers and types of miniature and micro-NIR spectrometers has been increasing in recent years. Some companies currently offering miniature equipment that has been tested on meat include Tellspec Inc., Consumer Physics (SCiO™), and Viavi Solutions Inc..

In the field of meat analysis, several labs have reported custom made equipment. Gentilin *et al.* (2016) and Zhang, Peng, Zhao, and Sun (2017) have both pursued prediction of moisture content, with the former developing a hardware/software platform with rapid response and a high signal to noise (S:N) ratio, and the latter developing equipment for use on the fresh meat conveyor line which, once triggered, will automatically make multiple measurements, dynamically display and then preprocess spectra, then generate predictions. Piao, Okura, and Irie (2018) reported on small portable equipment developed by them, then manufactured to be used under cold conditions for the prediction of fat quality, successfully transferring calibrations from a master unit to up to 5 slave units.

Moving towards miniaturization and/or reduced costs, Kandpal, Lee, Bae, Lohumi and Cho (2019) report the development of a system based on a monochrome camera and multiple LEDs spanning

458-950 nm for rapid evaluation of fresh meat quality. Some researchers have been working with the reduction of full spectra wavelengths to only those of importance to meat. Habib and Ullah (2016) performed computer simulation and testing of NIRs bandpass filters, specifically for regions important to meat classification or meat quality determination, that block wavelength contamination which would otherwise occur from the Distributed Bragg Reflectors (DBR) stopband. In an alternative solution to the DBR stopband restrictions, Ullah, Butt, Fomchenkov, and Khonina (2016) has reported filters composed of indium phosphide (InP) and air-gap layers to replace the alternating InP/SiO layers of the of DBRs of the Fabry-Pérot filters in miniaturized spectrometers in the 930-1450 nm range which is commonly used for meat.

3.2. HSI

The HSI technique is based on collecting and processing information from across the electromagnetic spectra. Hyperspectral devices marge the whole advantages of spectroscopy with the advantages of spatial information of surfaces (Amigo, 2020). Thus, they can be defined as fast and non-destructive instruments able to characterize sample from a chemical (chemical interactions) and physical (properties of the surface) point of view, after the proper data collection and analysis.

Nowadays, there are different commercial hyperspectral cameras, and their technology is continuously advancing in terms of acquisition speed and spectral/spatial resolution.

Even if there are different commercial HSI instruments, their setup is based on the interaction light-matter, or better, on the interaction between photons (with a specific energy and trajectory) with molecules of the sample understudy (Weisskopf, 2010). Thus, the instruments are mainly composed by a light source, a set of optical lenses, a wavelength dispersive device and a detector.

The photons are emitted by the light source (halogen lamps, LEDs or lasers) which should emit in the spectral range of interest, with high energy, without effects on the sample and guaranteeing illumination homogeneity (Amigo & Grassi, 2020). The latter is often achieved by light sources forming a 45° angle with the sample.

Most of the HSI systems take advantages of the reflection and transmission phenomenon to collect information about the chemical and physical properties of a samples. Indeed, when a photon striking a molecule, its energy is absorbed only if it has the same vibration frequency of the electron of the molecule. In case the frequencies of the photon waves are not the same than the natural frequencies of the molecules of the sample, they are reflected or transmitted. They are reflected in case molecules are “opaque” to those frequencies, which means that, when interacting with the matter, the electrons of the molecules on the sample surface vibrate just for short periods before allowing the photon with different energy to arrive to the detector. Depending on the properties of the molecules, as well as the

physical characteristics of the sample, the photon can be reflected in a specular mode (the same angle than the incident) or in a scattered mode (different angle than the incident). The photons are transmitted in case they hit "transparent" molecules, a.k.a. the vibrations pass through the matter and are reemitted on the opposite side of the object and reach the detector (Abbott, 1999).

After the emission, before or after interacting with the sample, the radiation is dispersed into narrow wavelength bands which are recorded individually by the detector. Among the wavelength dispersive devices, the most common are variable and tunable filters, imaging spectrographs and Fourier-Transform spectrometers (Amigo & Grassi, 2020).

At the end of the acquisition procedure the detector collects the coming incident light and convert it into electrical signals. Even if present in the market with different variation in the architecture and composition, mainly charge-coupled devices (CCDs) and the complementary metal-oxide-semiconductor detectors (CMOS) are implemented in HSI cameras (Amigo & Grassi, 2020).

3.3. NMR

In NMR, and also in MRI, the signal is produced by excitation of the nuclei of the samples with radio waves into nuclear magnetic resonance. High (HF) or low field (LF) NMR systems can be used for analyzing fresh meat. The LF-NMR systems generate magnetic field between 0.15 and 0.50 T. These systems are cheaper than the HF-NMR ones and do not have maintenance costs. However, their obtained spectra are of lower quality and sensitivity than those from HF-NMR systems, which generate magnetic field higher than 2T. However, HF-NMR systems are very expensive and require high maintenance costs, since they need to be cooled with helium or liquid hydrogen (Feig, 2011). The radiofrequency (RF) for LF-NMR systems is between 30 MHz and 100 MHz, and in HF-NMR system, it is higher than 100 MHz. Besides the type of magnetic field, there are several types of antennas oriented to excite the spin of different isotopes of chemical elements (Hornak, 1997), being ^{1}H the most used. And the spectra can be weighted on two different relaxation time: T1 and T2. T1 spin relaxation time (spin-lattice relaxation time) is the time from the longitudinal magnetization of the molecule of the sample from which the spectra will be obtained until their equilibrium value has been reduced by an "e" factor. T2 spin relaxation time (spin-spin relaxation time) describes the same process for the transverse magnetization. In this case, T2 is always smaller than T1, although both processes happen simultaneously. As acquisition sequence, most studies have applied the Carr-Purcell-Meiboom-Gill sequence (CPMG) that allows measuring relaxation times intensity of any nucleus (McIntosh, 2013).

3.4. MRI

The MRI acquisition in fresh meat has been carried out by using HF and LF scanners. HF MRI scanners offers images with a high quality, however, they are very high-priced and involve high maintenance costs (Feig, 2011). The LF MRI scanners are cheaper and do not require maintenance costs, but they have lower S:N ratio and, consequently, their images are of lower quality than those from the HF MRI ones. Among the obtained publications on MRI for this revision, most of the studies carried out in meat with HF MRI scanners have analysed dry-cured hams, there being a low number of works focused on fresh meat. However, the use of LF MRI scanners to analyse fresh meat is higher and it has experimented an increase in the last years.

For MRI, besides the type of magnetic field (HF or LF), the antenna, the relaxation time and the acquisition sequence are critical parameters for the image acquisition. The antennas that excite ^{1}H are the most used in meat (Pérez-Palacios, Caballero, Antequera, Durán, Ávila, & Caro, 2017). Nevertheless, some studies have also been carried out with antennas that excite ^{23}Na (Hansen, Van Der Berg, Ringgard, Stodkilde-Jorgensen, & Karlsson, 2008; Vestergaard, Risum, & Adler-Nissen, 2005), which are more specific for determining the salt content in meat and meat products. T1 is the spin relaxation time usually applied in most studies (Pérez-Palacios *et al.*, 2017). Different acquisition sequences can be selected, such as Multi-Slice (MSE), Inverse-Recovery (STIR), Gradient Echo (GE), Spin Echo (SE) or Volumetric (T3D), among others. Moreover, the echo time (TE) and the repetition time (RT) must be set for the image acquisition. TE is the time from the center of the radio frequency pulse to the center of the echo, and RT represents the length of time between corresponding consecutives series of pulses and echoes (Hendrick, 2005). SE sequences are characterized by long TE (around 20-30 ms) and short RT (less than 800 ms) and present a high S:N, while GE sequences have short TE (12 to 20 ms) and long RT (between 1200 and 2500 ms), with a lower S:N than SE. T3D sequences are a special GE sequences with 3D reconstruction, with a similar TE than GE and a very short RT (between 30 and 100 ms) (Ávila, Caballero, Antequera, Durán, Caro, & Pérez-Palacios, 2018; Caballero *et al.*, 2017a). SE is the most used sequence acquisition in the MRI studies of meat, while GE and T3D have been recently proved (Pérez-Palacios *et al.*, 2017).

Coils are also supporting elements to receive the MR signal. They have to be placed as near as possible to the area to be scanned. Coils can be classified as a function of their shape, volume or surface coils, or of their technology, linear or quadrature coils. In the case of musculoskeletal systems, the use of volume and quadrature coils, which surround almost completely the scanned area and receive the signal through two orthogonal channels, respectively, is the optimum combination. The size of the coil is also considered in the MRI studies in meat, using body coils for hams and carcass and hand/wrist, head or knee coils for smaller samples such as pork loins or chicken breast (Perez-

Palacios, Antequera, Durán, Caro, Rodríguez, & Palacios, 2011; Bernau *et al.*, 2015; Frelka *et al.*, 2019).

4. DATA ACQUISITION AND ANALYSIS

4.1. NIRs

Successful and reliable data acquisition must take into account equipment, environment, and sample condition. Firstly, a measurement method appropriate to the sample preparation must be chosen, then the equipment be calibrated. The most common measurement methods, shown in Figure 1, are reflectance (R) where most of the recorded light is reflected directly from the illuminated surface, or transmittance (T) where the light which travels through the sample is recorded. Both can be converted to absorbance for data analysis following a log transformation (log 1/R or log 1/T; Cortés, Blasco, Aleixos, Cubero, & Talens, 2019); interactance, records the light reflected from the interior of the sample and often uses fiber optics for illumination and detection as they can be placed in direct contact with the sample; and transflectance, in which light travels through the sample, encounters a reflector, then travels back through the sample before detection (Alander, Bochko, Martinkauppi, Saranwong & Mantere, 2013). Reflectance and interactance require thick samples to accommodate the long travel distances of NIRs wavelengths, while transmittance and transflectance require thin samples to facilitate sufficient light travel through the sample. In all cases, meat fiber direction should be consistent among samples. Long-standing do's and don'ts for equipment and sampling (Williams & Norris, 2004) include keeping equipment temperature constant, and operating under similar relative humidity during each data collection session to keep the amount of noise in the spectra similar for all samples. Samples may be homogenized, minced or ground, or intact, and of a thickness appropriate to the measurement method. Sample temperature must be consistent to prevent alterations to the spectral baseline and position of absorption bands. If samples have been dehydrated, measures must be taken to ensure moisture level is similar in all before reading. Sampling must be done to truly represent the subject, thus intact samples may require multiple reading locations; fiber orientation may be of importance for fresh intact meat samples. A recent review by Pasquini (2018) fully addresses NIRs fundamentals, chemometrics, and instrumentation while Xu, Xie, and Ying (2019) focus on identifying error sources.

The most common approach to analysis of NIRs spectra is pre-processing followed by processing. The pre-processing may be accomplished in a number of different ways and generally involves removal of noise at spectra extremes, further noise reduction over the remaining wavelengths (smoothing), and scattering and slope corrections. The lowest S:N is usually found at the extremes of the spectra, which is often removed simply by clipping the spectra. In the remaining body of the

spectra where S:N is higher, correction of scattering due to physical structure variations of the sample is usually performed with Multiplicative Scatter Correction (MSC), while Standard Normal Variate (SNV) is performed to correct spectra slope.

Reduction of random noise is often achieved by smoothing with a least squares polynomial fit, or in combination with 1st or 2nd derivative transformation, a method established by Savitzky and Golay (1964), although some authors have chosen to use Extended MSC (EMSC), such as Andersen, Veiseth-Kent & Wold (2017) who explored the effect of pH-related changes in extracted pork myofibrils as part of an equipment comparison study. Prevolnik Povse *et al.* (2017) and Soladoye *et al.* (2018) both used SNV and Detrend (SNVD), the former for quality prediction in intact pork fat layers and homogenized pork lean (n=56-130), and the latter for overall pork belly firmness from intact pork fat layers and lean (n=198).

By far, the most common processing approach for data exploration is principle component analysis (PCA) followed by regression or classification algorithms depending on the purpose of the study. In the case of regression, which is quantitative analysis, partial least squares (PLS, or PLS regression (PLSR)), is frequently used. All but two of the studies in Table 1 reported using this approach. Perez-Palacios, Caballero, González-Mohíno, Mir-Bel, & Antequera (2019), preferred to use the simpler algorithm, multiple linear regression (MLR), when predicting texture-related characteristics of pork loin cooked sous-vide at 70°C for 1, 2, 4, 6, or 8 h. In the case of classification, Moran, Andres, Allen, & Moloney (2018) whose research is discussed in more detail in 'Section 5.1 NIRs', used PLS discriminant analysis (PLS-DA).

Some recent alternative data analysis approaches in the meats field have included pre-processing synchronous 2D correlation spectroscopy to identify the key wavelengths, which were then used in SVM models (Wang, W., Peng, Sun, Wei, & Zheng, 2018a), and multi-index statistical information fusion (MISIF) for variable selection, (Qu *et al.*, 2018). Wu, Zhong, and Yang (2018) chose to forego preprocessing and instead establish a prediction model for freshness by using a double-layer stacked denoising autoencoder neural network (SDAE-NN) algorithm, which proved to out-perform PLSR and back propagation neural network (BP-NN). Processing has been approached by using combined stacked interval partial least squares (siPLS) and sparse partial least squares regression (SPLSR) to create stacked interval sparse PLSR (sisPLSR), which aims to "find favorable rotations of the classical PLS solutions while also utilizing local information in a spectra" (Poerio & Brown, 2017). Harrington (2018) modified an algorithm for training a restricted Boltzmann Machine, a type of neural network, to improve PLS calibrations for moisture, fat, protein.

4.2. HSI

Before sample acquisition, HSI systems should be calibrated for spectral and spatial information. The spectral calibration is performed with a black and a background reference as for spectroscopic devices. In detail, an image of the dark response is recorded by turning off the light sources or covering the lenses with non-reflective opaque black cap, thus, obtaining a 0% of reflectance image; and an image of the background response is recorded by a high reflectance standard or a spectra with 100% reflectance (ElMasry and Sun, 2010). Moreover, a spatial calibration is needed to set the ground coordinates (X-Y spatial directions) of the measuring scene by a printed checkerboard.

The proper acquisition mode is fundamental to obtain reliable results when performing an HSI analysis of sample, as it is for all the considered non-destructive techniques. There are different system configurations according to the procedure of image acquisition: spectral scanning (area scanning), spatial scanning (point and line scanning), and snapshot imaging (Qin, 2010).

In spatial scanning system, the intensity spectra of one or multiple spatial positions are acquired. In the case of one-point scanning, so called whisker-broom imaging, the spectra of each single pixel is acquired at a time by moving the sample in the measuring position which will have constant lighting path and diffusion (Figure 2.a). Actually, it will be the HSI systems more similar to normal spectrometers. The light source, the lens, the dispersive device (normally prism or optical gratings) and the line detector array remain fixed in a position, whereas the sample is moved systematically in two spatial dimensions.

The main advantages are the constant lighting path between the optical system and the sample and the high spectral resolution; resulting, however, in time-consuming measurements.

In the case of multiple spatial position scanning, so called line scanning or push-broom imaging, the intensity spectra of a portion of the sample is acquired at a time (Figure 2.b). Actually, a set of pixels dispose in a line (2-D spatial-spectral information) is acquired and then the sample is moved in just one direction, which normally is transverse to the slit.

The setup of those systems requires two-dimensional dispersing element (normally prism or optical gratings) and a two-dimensional detector array perpendicular to the surface of the sample.

Nowadays, these systems are the ones preferred for benchtop instruments applied for research purposes, but their setup is promising for industrial applications; indeed, they reach spectral resolution comparable to point scanning instruments, being faster up to one hundred times (ElMasry, Mandour, Al-Rejaie, Belin, & Rousseau, 2019).

The most common spectral scanning setups are area or plane scanning, which collect a global spatial information one single wavelength at a time. In this configuration, the whole system remains in a fix

position; i.e. the camera, the lens, the dispersive device and the field of view of sample location are in plane parallel to the detector (Figure 2.c). The main advantage of these systems is the affordable prize, the speed of acquisition; however, they normally return poor chemical information, with exception of cameras implemented with acousto-optic tunable filters (AOTF), which allows to acquire a higher wavelengths respect to variable filter ones. Their application for HSI benchtop instruments is not common, even though they are gaining importance in microscopy (Gottschall, Meyer, Schmitt, Popp, Limpert, & Tünnermann, 2018), as biological samples could be sensitive to the heating produced by the source lamps.

The last step of HSI acquisition is the file storage in the so called hyperspectral datacube, i.e. a 3D matrix in which along the 2D matrix (m rows and n columns) are stored the two orthogonal spatial directions and along the third dimension is store the spectra information (λ). There are different ways to ordered in a logical manner the collected spatial and spectral information, such as band interleaved by pixel (BIP), by line (BIL) and band sequential (BSQ). Dedicated software allows the proper management of the datacube, whichever is the storage format, for further data analysis.

As discussed previously, the result of HSI analysis is an image with spectral information combined with spectral information stored in each pixel. The large amount of data and their high correlation need a proper handling to extract the relevant results by the adaptation of the multivariate data analysis techniques. In this section the steps required previously to multivariate data analysis performance are discussed, indeed, there are different "cleaning" procedures to properly pre-process the acquired images for discarding erroneous data values and non-informative background. For more detailed information, refer to Vidal & Amigo (2012).

The determination of dead pixels and spikes is fundamental to get rid of spurious information which may affect the performance of multivariate data analysis techniques.

Dead pixels are those pixels with missing or zero values and can be isolated or grouped in a specific location (line or area) of the image as they result from anomalies of the HSI detector. Several techniques are present in software dedicated to image analysis (Mobaraki & Amigo, 2018), such as thresholding techniques from median spectra calculated from the data, or more robust methods like genetic. Once located they are normally corrected by interpolation (by mean or median) with neighbour pixels ensuring a good representation of the information, as the neighbour pixels are generally highly correlated.

Other failures to be detected, and corrected accordingly, are rapid and sharp rise-fall of the signal, defined as spikes, resulting from failures of the detector or of the electronic circuits. Even if it is quite simple to detect spikes by visual inspection of the spectra, there are several approaches which can be

used to automatically correct them in huge dataset as the ones generated by HSI. For a comprehensive revision refer to Vidal & Amigo (2012).

Most of the time the acquired HSI is not containing just the information of the sample understudy but it covers all the scanned area; thus, this area should be discarded. The more direct, but tedious and long, strategy is the manual selection of the sample area by image visualisation at one, combine or whole spectral variables or by visualization of the scores image obtained by after a PCA. From the same visualisation (wavelength or scores) a threshold value, defined manually or by histogram inspection, can be applied to discriminate the sample from the background. Anyway, it should be considered that thresholding is always a critic point in image analysis as it could be affected by many factors, mainly the type of data and the personal experience.

After the mentioned "cleaning" procedures the data stored in as HSI are normally pre-treated and analyzed adopting the techniques of classical spectroscopy, including clustering, classification and regression methods.

4.3. NMR

Prior to analyze the spectra acquired from the NMR systems, it must be pre-processed. For that, firstly, the chemical shift misalignment must be corrected by using shifting algorithms, being the most commonly applied the icoshift algorithm (Savorani, Tomasi, & Engelsen, 2010). This algorithm optimizes by shifting of spectral intervals, aligning the peaks of the spectral intervals and the spectra simultaneously. For that, correlations among the spectral data are used. After that, the noisy regions must be removed and then, NMR spectra must be normalized and scaled (Craig, Cloarec, Holmes, Nicholson, & Lindon, 2006). These algorithms allow increasing the representation of lower concentrations and minimizing the contribution of noise. Finally, some pre-processing techniques in classical spectroscopy are applied, being the most used the algorithms: Savitzky-Golay that aims to reduce the noise of the spectra, which is often achieved by smoothing algorithms in combination with 1st or/and 2nd derivative transformation; Standard Normal Variate (SNV), which aims to correct the slope of the spectra in order to optimize the spectral data; Multiplicative Scatter Correction (MSC), which aims to correct the scattering due to external interactions with the sample, i.e., lights, temperature,... (Rinnan, Van Der Berg, & Engelsen, 2009). As example, Figure 3 shows a NMR spectra of beef. Then, for extracting the data from the spectra, the identification of each peak is related to each component of the sample. For that, the MMCA (Metabolite-Metabolite correlation analysis) is commonly used to identify the component of each spectra (Craig *et al.*, 2006). Finally, the intensity of each peak is measured as concentration value of each component.

For the data analysis, in general, Partial Least Square (PLS), Principal Component Analysis (PCA) or Multiple Linear Regression (MLR) have been usually applied in order to obtain accurate results in NMR.

Other statistical tools such as ANOVA, Pearson's correlation coefficient, Naïve-Bayes, first-order and second-order statistics have been applied for analyzing the data obtained from the spectra (Delorme, Sejnowski, & Makeig, 2007). From all these statistical techniques, PCA must be noted. PCA is the most used exploratory data analysis technique, since it is usually used to identify patterns in measured data and to visualize the distribution of the data. This technique allows evaluating the relationship among the variables by using mapping and displays techniques for understanding the structure of the complex multivariate datasets (Bro, & Smilde, 2014). PLS (Bro, 1996) aims to maximize the covariance between the predictor and the response data. Its popularity can be ascribed, in part, to its speed, since the model parameters for each component can be calculated easily. Its ease of use because of the only meta-parameter to be optimized is the number of components. Its interpretation since the PLS scores, loadings and weights can be investigated in order to determine whether the model components have a meaning for the meat and meat products (Martens, & Naes, 1989). MLR is used to represent linear relationship between a dependent variable and several independent variables. This technique obtains a linear regression equation, which can be used to predict future values (Hastie, Tibshirani, & Friedman 2001).

4.4. MRI

Once the MRI image has been acquired, it is analysed to extract numerical information. Pre-processing and/or segmentation techniques are firstly applied. The objective of the pre-processing is to improve the obtained image by outstanding certain features or eliminating noise (Sonka, Hlavac, & Boyle, 1999). The segmentation techniques extract elements of interest from the images (Maravall, 1993), such as the thresholding methods (Cheriet, Said, & Suen, 1998; Otsu, 1979) or fuzzy logic (Raof *et al.*, 2008). Other applied segmentation techniques in MRI from meat are active contour, which detect the muscle of interest (Caro, Rodríguez, Cernadas, Durán, & Villa, 2001; Caro, Rodríguez, Durán, & Antequera, 2012), and the algorithms for selecting region of interest (ROI) (Molano, Rodríguez, Caro, & Durán, 2012), which is the maximum area inscribed in the muscle previously selected. The last step of the image analysis is the extraction of the computational characteristics. This process allows describing the MRI as a vector of features. For this task, algorithms based on texture features have been the most used: Gray-Level Co-occurrence Matrix (GLCM), Gray-Level Run Length Matrix (GLRLM) and Neighbouring Gray-Level Dependence Matrix (NGLDM). GLCM counts the number of times that each pair of gray levels (i,j) occurred at a

given distance *d* in all directions. GLRLM measures runs into the image, i.e., a set of consecutive pixels in the image with the same gray level value. NGLDM considers the relationship between an element and all its neighbouring elements at one time rather than one direction at a time. The application of these algorithms results on the values of different computational texture characteristics.

The use of fractal algorithms for analysing MRI from meat has been recently studied. They study the degree of symmetry or self-similarity found in a structure at all scales, allowing the identification of recurring patterns and removing the possibility of image compression (Hibbert, 1991). Three fractal algorithms have been used in meat: the traditional algorithm to compute the fractal dimensions, the fractal texture algorithm (FTA) and the one-point fractal texture algorithm (OPFTA). The traditional algorithm measures the number of boxes (small fractions of the image depending of the size of the original image) needed to cover an area occupied by the object as a function of the size of boxes. FTA (Caballero, Caro, Ávila, Rodríguez, Antequera, & Pérez-Palacios, 2017b) is a novelty texture algorithm based on the number of times that a pattern is repeated in each image depending of box size calculated in each case. These fractal features are gathered in a vector, and each vector was computed based on second order statistics. OPFTA (Caballero *et al.*, 2018) is an algorithm based on features obtained from fractal properties values into smaller rectangles of 32x32 pixels. From all these values, the value for the box size equal to eight is selected. After that, these values are gathered in order to create a matrix, so, each cell of the matrix represents one ROI from the image. Finally, the features were calculated on the matrix by applying second order statistics.

Other algorithms to analyse the MRI images of meat are the mapping techniques (Zarei, & Sepyani, 2016), the use of contrast on the images (Vala, & Baxi, 2013), the histograms (Bajd, Skrlep, Candek-Potokar, & Sersa, 2017), and the 3-D version of the texture (Ávila, Caballero, Durán, Caro, Pérez-Palacios, & Antequera, 2015). The mapping techniques is based on geometric transformation of images, re-locating the points in the source images on different coordinates in a destination image. This allows describing some features of the images (Zarei, & Sepyani, 2016). The contrast on the images stands out some zones of the images. The use of this technique joins to the thresholding methods allow describing some features of the images and characterize them (Vala, & Baxi, 2013). The 3D version of the texture algorithms has also been applied for the analysis of 3D reconstructed MRI images (Ávila *et al.*, 2015).

Regarding the data analysis, in the case of MRI, most studies have applied usual statistical tools such as Pearson's correlation coefficients, analysis of variance (ANOVA), PCA or statistics measurements as the first and second order statistics. In the last years, the application of data mining in these studies has increased. Data mining is one of the steps of a larger process known as Knowledge Discovery in

Databases (KDD) (Fayyad, Piatetsky-Shapiro, & Smyth, 1996), and it is related to large volume of data. Most of the data mining techniques applied in the MRI studies of meat are MLR and Isotonic Regression (IR). IR estimates ordered values for an independent variable as a function of one of the input variables (Barlow, Bartholomew, Bremner, & Brunk, 1972), only selecting the input parameters with the best adjustment results. Partial Least Square (PLS) has also been applied the MRI studies in meat.

Most of the MRI studies based on regression methods have applied the common cross-validation methodology (Kohavi, 1995), which divides the data in two sets, training and testing, with information of images from the same sample. Recently, a modified of the usual method has been developed. It consists of three sets (training, validation and test) and leaving one meat piece out when creating the dataset (Ávila *et al.*, 2019).

5. APPLICATIONS OF NON-DESTRUCTIVE METHODOLOGIES FOR FRESH MEAT ANALYSIS.

5.1. NIRs

Since the excellent and comprehensive reviews by Dixit *et al.* (2017), Kademi, Ulusoy, and Hecer, (2019), and Prieto, Pawluczyk, Dugan, and Aalhus (2017), there have been roughly 6 types of NIRs studies, depending on their objective, that have analysed fresh meat in the last 4 years. The first type of study used NIRs as a standard laboratory method. Konarska, Kuchida, Tarr and Polkinghorne (2017) used correlation analysis to compare three approaches to measuring beef marbling on 12 muscles: image analysis, and subjective evaluation from images of the intact sample, and NIRs on the homogenized sample using the NIRFlex N-500 (Buchi, Switzerland) with its built-in prediction algorithm. The overall strength of correlation for % marbling between NIRs and image analysis was 0.60 ($P \leq 0.01$) while for individual muscles it varied from 0.13 (*gluteus medius*) to 0.77 (*serratus ventralis cervicis*; ≥ 0.56 significantly different from 1 at $P \leq 0.01$). Mínguez, Sánchez, Hernández, Ragab, El Nagar and Baselga (2017) used NIRs to predict fatty acid composition and % protein from crossbred ground freeze-dried rabbit *longissimus lumborum* in order to evaluate the genetic groups used in the crossbreeding and to estimate genetic contributions to meat quality. A difference in fatty acid composition ($P \leq 0.05$) was detected for one genetic line, but no differences in % protein. The second type of study used NIRs for authentication. Moran *et al.* (2018) tested various pre-processing approaches to confirm degree of ageing of three different, intact, bloomed, beef muscles following 3, 7, 14 and 21 d of vacuum-packaged storage. In this preliminary study, it was found that the best prediction model was specific for each muscle, and was best following spectral pre-treatment such as Savitsky-Golay 1st or 2nd derivatives on the full spectra (400-2400 nm). When tested, model

sensitivity ranged from 96.3-100%, specificity from 98.8-100%, and overall correct classification from 99.1-100%. Pieszczek, Czarnik-Matusewicz, & Daszykowski (2018) explored two class modelling techniques: one-class classifier partial least squares (OCPLS) and soft independent modelling of class analogy (SIMCA) to recognize pure minced beef, pork, or lamb from NIRs spectra. For beef, models offering the best performance, with an emphasis on specificity, were either SIMCA preceded by SNV (sensitivity = 99.8% ± 0.78; specificity = 98.98% ± 0.56) or OCPLS preceded by MSC (sensitivity = 99.11% ± 5.07; specificity = 99.9% ± 0.37). SIMCA performed best for pork and lamb, with no pre-processing for the former (sensitivity = 99.94% ± 0.49; specificity = 87.20% ± 4.00), and preceded either by MSC (sensitivity = 99.98% ± 0.20; specificity = 98.00% ± 0.58) or ISC (sensitivity = 99.48% ± 0.79; specificity = 99.06% ± 0.47) for the latter. Table 1 summarizes the 4 other types of studies along with their calibrations and performances: detecting adulteration, prediction, equipment testing, and exploration into various spectra pre-processing and processing approaches.

Prediction studies have been diverse (Table 1). Li, Z., Jia, Wang, Liu and Dong, (2016) reported predicting cooked beef texture from the raw meat. Pork studies include prediction of pork components with particular emphasis on fat composition (Richli, Kaufmann & Scheeder, 2016; Prevolnik Povse *et al.*, 2017), identifying potential PSE (Li, X. *et al.*, 2016), determining cholesterol levels (Wang, H. *et al.*, 2017), post mortem meat quality (Andersen, Wold, Gjerlaug-Enger & Veiseth-Kent, 2018a) and belly firmness (Soladoye *et al.*, 2018). Lamb studies looked at lipid peroxidation to replace TBARS (Ripoll, Lobón & Joy, 2018), and classification for eating quality (Knight *et al.*, 2019). Equipment used was a mix of benchtop and portable, and usually intact samples were tested. The wavelength range was more frequently VIS-NIRs than NIRs alone. Pre-processing commonly consisted of smoothing, 1st or 2nd derivative, and SNV, while processing was always PLS or PLSR.

NIRs is a growing field, therefore new equipment is continuously under development. There have been a number of reports on testing results in recent years. Dixit and his research group have reported a group of studies centering around equipment developed in–house, and which consists of a Fabry-Pérot interferometer, a 4-point photodiode array, and collimating lenses, enabling multipoint data capture (Dixit *et al.*, 2016a; 2016b; 2016c). The equipment has been designed for rapid on-line detection and prediction of ground meat composition, thus performance has been reported for different sample stand-off distances, movement speeds, and combinations of both. Several equipment testing reports were based on technology comparisons (eg. NIRs, hyperspectral imaging (HSI), Fourier transform-NIRs (FT-NIRs), Raman, fluorescence, etc.), and the NIRs results can be found in Table 1 (Andersen *et al.*, 2017; Andersen, Wold, & Veiseth-Kent, 2018b; Nolasco-Perez *et al.*, 2019).

Piao *et al.* (2018) explored the efficacy of transferring calibration equations for beef fatty acid groups developed on master equipment, to slaves. Wang, W., Peng, Sun, and Li (2017) tested custom in-house equipment constructed of two spectrometers with different wavebands, operated in sequence, for the ability to predict pork freshness on a conveyor line. This team also explored different data pre-processing and processing approaches (Wang, W., Peng, Zheng, Tian, & Wei, 2016; Wang, W., Peng, Sun, Zheng, & Wei, 2018b) and included reducing the spectra to key wavelengths to potentially increase the rate of data collection (Wang W., *et al.*, 2018a).

5.2. HSI

Hyperspectral imaging for the assessment of meat quality by chemical composition has been applied mostly for moisture, fat content and composition and protein. Also, and Total Volatile Basic Nitrogen (TVB-N), TBARS and K-value have been investigated as quality indexes for meat freshness evaluation. As concern technological and sensory attributes, WHC (water holding capacity), WBSF (Warner–Bratzler shear force), SSF, (slice shear force) and colour by CIE - Lab* chromatic scale have been considered. Thus, the works dealing with their determination by HSI are here revised (Table 2), excluding reference dealing with microbiological quality determination; in case of interest in this field please refers to the review by Kamruzzaman, Makino, and Oshita (2015).

Different line scanning approaches (or push-broom imaging) have been proposed for moisture content determination. Kandpal, Lee, Kim, Mo, and Cho (2013) proposed a VIS/NIRs – HSI system ranging from 400 to 1000 nm to predict moisture content in chicken breast. 52 samples were used to calibrate the PLSR model, whereas other 20 chicken breasts were used to validate the model reaching optimal levels (R^2_P of 0.94 and SEP of 0.71%.) when only the NIRs (700-1000 nm) range was used. The laboratory-based push-broom NIRs hyperspectral imaging system (900–1700 nm) proposed by Barbin, ElMasry, Sun, and Allen (2013) allowed the construction of good PLS regression models, developed from feature-related wavelengths, to predict moisture content in minced pork samples (R_P of 0.91 and SEP of 0.62). The same research group developed moisture content prediction models for fresh minced beef samples collected from different muscles reaching prediction abilities for R_P of 0.89 and accuracy (SEP) of 0.46 (ElMasry, Sun & Allen, 2013).

By a larger NIRs range (880 – 1720 nm), Zhao, Esquerre, Downey and O'Donnell (2017) demonstrated higher prediction ability for moisture content in ground beef samples (R^2_P of 0.99; RMSEP of 0.64 w/w). However, the samples used by Zhao *et al.* (2017) to calibrate (n=36) and validate (n=9) the model were quite small compared to Barbin *et al.* (2013) and ElMasry *et al.* (2013), both considering around 80 samples for the training set, and 40 samples for the testing set.

Also lamb meat has been tested for moisture prediction by push-broom hyperspectral imaging system in the spectral range of 900–1700 nm (Pu, Sun, Ma, Liu & Kamruzzaman, 2014). In their study a relevant number of samples has been used, being 127 lamb meats including *semimembranosus*, *semitendinosus* and *longissimus dorsi* muscles. Results comparable to those of Barbin *et al.* (2013) and ElMasry *et al.* (2013) have been obtained by applying MLR models after a hierarchical variable strategy (UVE-SPA-CSA), being the R_P of 0.92, the RMSEP of 0.58 and the RPD equal to 2.53.

Fat content as total amount, intermuscular fat (IMF), or specific classes composition (SFAs, saturated fatty acids; UFAs, unsaturated fatty acids and oleic acid) have been widely investigated across different meat species.

The study by Wold, O'Farrell, Høy, and Tschudi (2011) revealed how simplified HSI instrument (multispectral imaging system with 15 wavelengths between 760 and 1040 nm) can be used for the online estimation of fat content in beef trimming. Indeed, they reached high fat prediction accuracy (RMSEP of 0.6%) in 100 batches. More recently, Lohumi, Lee, Lee, Kim, Lee and Cho (2016) calibrated models for fat content in beef from different quality grades by ANOVA, spectral angle measure (SAM), and Euclidean distance measure (EDM) methods, reaching R^2_C of 0.91, 0.95, and 0.96 however, they used a small number of samples (n = 24) and they did not perform any validation using independent samples. By revising the last decade literature, it seems that the best model on term of prediction for fat in raw beef samples was develop by Zhao *et al.* (2017); they obtained R^2_P of 0.99 and RMSEP of 0.73% w/w of fat by applying EMCV-PLSR algorithm. Similarly, Pu *et al.* (2014) developed MLR models after a hierarchical variable strategy (UVE-SPA-CSA) obtaining R_P of 0.98, RMSEP of 0.36 and RPD of 4.13. The strength of their work over Zhao *et al.* (2017) is due to the high number of samples and they representability as they considered 126 lamb meats including *semimembranosus*, *semitendinosus* and *longissimus dorsi* muscles (84 samples used to calibrate the model and 42 for its independent validation).

The research group by Kobayashi developed models for the prediction of specific fat categories in beef samples (Kobayashi, Matsui, Maebuchi, Toyota & Nakauchi, 2010 and Kobayashi, Mori, Nishino, Toyota & Nakauchi, 2012). They obtained reliable models for the prediction of saturated fatty acids (R^2_P = 0.87, RMSEP =1.69, RPD=2.43), unsaturated fatty acids (R^2_P = 0.89, RMP =3.41, RPD=2.84) and oleic acid (R^2_P= 0.71, RMSEP =3.13, RPD=1.855) by predicting at least 32 meat samples from three 25-month-old Japanese Black (Wagyu) cattle.

Both Liu and Ngadi (2014) and Huang, Liu and Ngadi (2017) developed regression models to predict IMF in porcine meat by combining different image features – from WLD to Gabor filter and improved GLCM (gray level co-occurrence matrix) - with spectral information. Liu and Ngadi (2014) reached an optimal model performance in prediction with an adjusted R_P^2 and RMSEP of 0.93 and 0.17%,

respectively; whereas the rib by rib models developed by Huang *et al.* (2017) reached a R_P of 0.90 and an RMSEP of 0.92% for the 3rd last rib even if the model was constructed with only 18 samples and validated with 6.

A relevant study for IMF prediction was developed by Craigie *et al.* (2017). Indeed, they performed HSI acquisition of 2454 samples of lamb loin (*M. longissimus lumborum*) at processing plant level over consecutive years. They evaluated the performance of more than ten different regression algorithms reaching prediction abilities up to R^2_P of 0.72 and RMSEP of 0.45 with a Gaussian process regression (GPR) approach.

Prieto Osika, Aalhus, Lopez-Campos, Juarez, and Pawluczyk, (2018) reported that models based on HSI to predict protein are generally less accurate than the ones for moisture or fat. Indeed, Pu *et al.* (2014) only reached R_P of 0.67, RMSEP of 0.41 and RPD of 1.31 when predicting protein content by the UVE-SPA-CSA-MLR model calibrated with 126 lamb samples. Certainly, the estimation of protein content by HSI data seems highly dependent on the sample form: models developed based on minced meat generally reached higher performances over intact muscles analysis. This is proved by the studies of Kamruzzaman, ElMasry, Sun and Allen (2012a) and ElMasry *et al.* (2013). The latter developed models for protein prediction in beef samples from three different muscles (M. *longissimus dorsi, M. semitendinosus* and *M. psoas major*) reaching high performance (R^2_P of 0.86, SEP of 0.29) and for pork samples reaching R_P^2 of 0.88 and SEP of 0.40. It has been hypothesized that homogenized samples, such as minced meat, overcome interferences of muscle fibre organization and muscle physical characteristics (Prieto *et al.*, 2018) leading to better prediction capabilities.

Khulal, Zhao, Hu and Chen (2017) developed models to predict TVB-N in poultry by back propagation neural network (BPNN) algorithm. They analysed fifty chicken breast fillets by an *ad hoc* developed hyperspectral imaging system and, by combining the spectral variables with the texture ones, they calibrated a good regression model, further validated by other 25 samples, reaching a R_P of 0.75, and a RMSEP of 6.39mg/100g of meat.

Great interest has been posed by the scientific community in predicting TVB-N in pork meat in recent years. Both Li, Chen, Zhao and Wu (2015) and Guo, Huang, Zhu, Guo and Qin (2018) developed methods based on NIRs-HSI systems based on line-scanning in the 400-1000 nm range to predict TVB-N in fresh pork. Even if they used different regression strategies, namely Least-squares support vector machine (LS-SVM) and Back propagation artificial neural network (BPANN), they were able to obtain optimal models in terms of coefficient of determination (R^2_P>0.93). However, the error (RMSEP) obtained by Li *et al.* (2015) resulted considerably lower (RMSEP= 1.86mg/100g) in respect to the one obtained by the BPANN model (5.52mg/100g).

Differently, Lee, Kim, Lee and Cho (2018) proposed the use of a hyperspectral fluorescence imaging system, based on high-intensity light-emitting diodes at 365 nm, for the determination of TVB-N contents in pork meat. In their work, 186 fresh pork *longissimus* muscles were purchased from a local supermarket, trimmed and shaped in size of 5cm x 4cm x 2.5cm to be analysed. The developed model was based on LS-SVM, leading to an optimal prediction capability (R^2_P of 0.967 and RMSEP of 1.90%).

As far as concern lipid oxidation, a research by Xiong, Sun, Pu, Xie, Han, and Luo (2015a) studied the possibility of developing a regression model based on HSI data to predict TBARS in chicken breast slices during storage at 4 °C for 0, 3, 6, 9 days. They established a simplified model by selecting 10 optimal wavelengths using the successive projections algorithm (SPA) able to predict TBARS with good performance, being the R_P of 0.80 and the RMSEP of 0.16 mg/100g.

Cheng, Sun, Pu and Liu (2016) proposed a feature level fusion of HSI spectral data and textural data to develop PLSR model for the prediction of another important freshness indicator of meat, K-value. They selected six feature wavebands (407, 481, 555, 578, 633, and 973 nm) and merged them with texture data of the grayscale images extracted by GLCM at the selected wavebands. The data fusion approach resulted in improved models with R^2_P of 0.92 and RMSEP of 4.0%.

If the success of HSI is expected for chemical composition analysis, its application for technological attributes has also been investigated - with more or less success - in the recent years.

Indirect measure of pH has been proposed for beef (ElMasry *et al.*, 2013), pork (Barbin *et al.*, 2012) and lamb (Kamruzzaman, ElMasry, Sun & Allen, 2012b). Even if applying different regression approaches models developed for beef and lamb did not performed well (R^2_{CV} lower than 0.70). The same authors hypnotised that the considered pH variation in animal flash after-post mortem process could be too small to construct a robust model. However, the model developed for pork gave R^2_P of 0.90 and RMSEP of 0.10, when considering a similar variation range was 5.31 – 6.43.

HSI systems demonstrated to be useful for colour determination intuitively when the spectral range covered also the visible part (400-700 nm). This is the case of the models developed by Wu, Peng, Li, Wang, Chen, and Dhakal, (2012) for beef and by Kamruzzaman, Makino, and Oshita (2016a) for beef, pork and lamb. Those models reached high prediction capabilities for a* determination, which describes the colour space from green (−) to red (+), thus, the expected variation in red meat. Also, models developed for L* - lightness from black (0) to white (100) – gave high predictive performances (R^2_P>0.96).

WHC modelling brought to heterogeneous results. Barbin *et al.* (2012) and ElMasry, Sun and Allen (2011) obtained good models after variable selection in prediction (R^2_P=0.89, RMSEP=0.79%) and cross-validation (R^2_{CV}=0.89, RMSECV=0.26%), respectively. The variable selection strategy (RC-

LS-SVM optimal wavelengths) resulted successful for the models developed by Kamruzzaman, Makino, and Oshita (2016b) leading to excellent WHC predictions and clear distribution maps for beef, pork and lamb samples. Less promising results were obtained by the authors using the full NIRs spectral range (Kamruzzaman *et al.*, 2012b).

Models based on HSI for the prediction of meat texture, highly relevant for consumer acceptance, has been recently investigated. For instance, Xiong *et al.* (2015b) achieved acceptable results (R_P of 0.87 and RMSEP of 0.05) by applying PLS regression to images collected in the Vis/NIRs-HSI range (400 to 1000 nm) to predict hydroxyproline in poultry meat. For extensive details about recent application of HSI for texture prediction in meat products refer to Reis *et al.* (2018).

5.3. NMR

Several studies have been found in the scientific literature by applying LF-NMR and HF-NMR systems to estimate quality traits of fresh meat (Table 3).

The use of LF-NMR to analyse pork samples was firstly tested with the aim of study the relationship between cooking temperature, the water distribution and some sensory attributes (Bertram, Aaslyng, & Andersen,, 2005). T2 as relaxation time and CPMG sequence for the spectra acquisition were applied, while PLS was selected for the data analysis. High correlation coefficients were found between the changes in the sensory attributes, which were caused by the temperature of cooking, and the spectral data, i.e. juiciness ($R^2 = 0.82$), tenderness ($R^2 = 0.87$)). Moreover, Straadt, Rasmussen, Andersen, and Bertram, (2006) demonstrated the relationship between the water holding capacity and the water distribution of loins with different days of aging while are cooking and the NMR data ($R > 0.75$). These authors used a LF-NMR system (23.2 MHz) with T2 relaxation time and CPMG sequence.

In the case of chicken samples, most studies used LF-NMR and T2 relaxation time. Thus, Li, Wang, Xu, Xing, and Zhou (2014) tried to determine the effect of freezing-thawing with different conditions of high pressure on water holding capacity or cooking loss of chicken by means of LF-NMR. These authors used CPMG sequence and applied correlation coefficients as data analysis technique. Thus, good to excellent but inverse relationship were found both parameters (water holding capacity R= -0.707, cooking loss R= -0.920). Under the same analytical conditions, previous studies had also found high correlation coefficients between T2 signal intensity and water activity ($R > 0.90$) (Venturi, Rocculi, Cavani, Placucci, Dalla Rosa, & Cremonini, 2007), cooking loss ($R = 0.986$) and moisture content ($R = 0.953$) (Shaarani, Nott, & Hall, 2006).

The use of LF-NMR has also been evaluated in beef. Pereira and Colnago (2012) determined the moisture content on beef samples by applying CPMG sequences weighted on transverse

magnetization relaxation time (T2) on LF-NMR (8.9 MHz), and using PLS and PCA as data analysis techniques. Correlation coefficients obtained between moisture content and T2 intensity values of NMR were higher than 0.96. Moreover, mixes of beef and horse were tried to be classified as a function of the quantity of each type of meat by LF-NMR (60 MHz). For that, T1 and T2 relaxation times were applied and PCA and Naïve Bayes statistics were used as classification techniques. Results showed that 106 of 107 samples were correctly classified, showing the accuracy of this methodology to differentiate mixtures of different meat (Jakes *et al.*, 2015).

The effect of thawing and post-thawing on a number of quality parameters of rabbit meat (lipid oxidation, water holding capacity, instrumental color and texture) has also been studied by applying LF-NMR (70 MHz) (Jia, Liu, Nirasawa, & Liu, 2017). For that, transverse magnetization relaxation time (T2) and CPMG pulse sequence were used on LF-NMR. ANOVA and correlation coefficients were applied as data analysis techniques. Correlation coefficients higher than 0.95 were achieved for all parameters studied in this work.

HF-NMR has not been highly used in fresh meat, with only a study being found in duck samples (Liu, Pan, Ye, & Cao, 2013). These authors evaluated the capacity of HF-NMR to discriminate meat samples as a function of the age of the ducks and to determine 22 metabolites. These authors used T1 relaxation time and CPMG pulse sequence on HF-NMR (400 MHz), and PCA and PLS as data analysis techniques. Results showed accurate classification results (percentage of correct classification higher than 60 %), differentiating among meat samples from duck of 27, 50, 170 and 500 days old, and correlations coefficients (higher than 0.70 for most metabolites).

5.4. MRI

Most of the MRI studies in meat have been published after the year 2000, and they have been mainly carried out by using HF scanners, being the dry-cured ham the most sampled meat product in this kind of works. However, the interest on LF-MRI is experimenting a significant increase nowadays.

Regarding the publications about the use of MRI to analyse fresh meat in the last years, which are summarized in Table 4, the earliest works (2011-2016) used HF-scanners, whereas LF ones have been preferred in the latest researches (2015-2019). It is also noted that these recent studies on MRI and fresh meat can be fairly gathered as a function of their main objective: classifying of the meat samples, analysing the percentage of intramuscular fat or lean, optimization of the MRI methodology to predicted the quality parameters of meat and evaluation of the changes due to freezing/thawing the meat samples.

Studies centred on classification purposes have been carried out with hams (Perez-Palacios *et al.*, 2011; Caballero *et al.*, 2016). These authors aimed to discriminate between hams from pigs fed with

different diets (acorn and grass vs. high oleic acid enriched feeding) (Perez-Palacios *et al.*, 2011), and as a function of their salt content (Caballero *et al.*, 2016). In both studies the images were acquired by using HF-H[1] MRI scanners with a quadrature whole-body coil and applying T1-weighted spin echo sequences. Three similar steps were carried out in both studies for the MRI analysis. Active Contours was applied on the images to recognize the *Biceps femoris*, in both studies, and the *Semimembranosus* muscles, only in the salt study. Then, the Region of Interest (ROI) was selected on each muscle. In the salt study, each ROI was divided into minor rectangles, which can be called mini-ROIs. Finally, the analysis of the ROIs and mini-ROIs was done by applying three computational texture algorithms (GLCM, GLRLM, NGLDM), obtaining a vector of 15-17 computation texture features.

Results obtained in the study of Perez-Palacios *et al.* (2011) showed visual differences between the MRI of hams from pigs fattened with acorn and grass (darker grey colour that represents the muscle) and high oleic acid concentrates (brighter white colour that represents the fat) (Figure 4). Besides, ANOVA showed statistical differences in the values of the texture features between the two batches and PCA displayed a clear separation of the two groups of hams.

In the case of the salt study, Caballero *et al.* (2016) applied classification techniques of data mining, getting a 77-79% of correct classification of ham muscles with different salt content when applying the J48 decision tree technique. These authors also achieved to predict the salt content as a function of the computational texture features with high accuracy by MLR.

As for the studies based on determining the content of fat and lean by MRI, Lee, Lohumi, Lim, Gotoh, Cho, and Jung, (2015) scanned different beef samples (ribeyes of four categories) by using a LF-H[1] MRI with a head coil and SE-T1 sequences. Then, the threshold method was applied to calculated total area of the image and of the intramuscular fat, as well as their number of pixels. The percentage of intramuscular fat was then calculated considering these data and the density of the fat and muscle = (total pixel number of intramuscular fat * fat density) / (total pixel number of muscle * muscle density) + (total pixel number of intramuscular fat * fat density) * 100. Results on this study were more precise for samples with high fat percentage than for that with low fat content, which authors have ascribed to thresholding method. It classifies each pixel as pure fat or not, but some pixel may contain both tissues.

In the same line, Bernau *et al.* (2015) investigated about the use of MRI to evaluate the carcass composition of boars, instead of the standard protocol. Samples were scanned in a LF-H[1] MRI with a large body coil and GE-T1 sequences. Images were analysed semi-automatically by the interactive segmentation function to separate muscles from fat and removing bone and cartilage tissues manually. Total volume and the volume of fat and lean were calculated on the different regions and muscles of

the carcass and compared with the results from the standard protocol. A stepwise regression analysis was carried out on these traits, resulting in a regression equation for the percentage of lean meat with a high coefficient of determination ($R^2 = 0.88$).

The principal objective of most studies using LF MRI scanners has been the optimization of the procedure to achieve high accurate results (Perez-Palacios *et al.*, 2017; Caballero *et al.*, 2017a; Ávila *et al.*, 2018). In these works, pork loins were scanned by using a LF-H^1 MRI with a hand/wrist coil. Different combinations of acquisition sequence, image analysis methods and prediction techniques of data mining techniques have been tested to reach the best option for predicting the quality characteristics of pork loins most precisely. Perez-Palacios *et al.* (2017) focused on the texture algorithms (GLCM, GLRLM, NGLDM), Caballero *et al.* (2017a) on fractal algorithms (CFA, FTA, OPFTA) and Ávila *et al.* (2018) on 3D texture algorithms (3D GLCM, 3D GLRLM, 3D NGLDM), whereas the same acquisition sequences (SE, GE and T3D weighted in T1) and data mining techniques (MLR and IR) were evaluated in the three works.

Perez-Palacios *et al.* (2017) observed visual differences in the MRI of loins depending on the acquisition sequence, with SE offering sharper and better-defined images than GE and T3D, and also found the significant influence of the acquisition sequence on the values of all computational texture features. Prediction equations of the different physico-chemical parameters analysed (percentage of moisture and lipid, water activity and instrumental colour coordinates) showed accurate correlation coefficients when applying SE or GE in combination with any of the acquisition sequences or data mining techniques tested, while the use of T3D sequence lead to less precise results. In view of that, it was considered the time consumed and the required resources to choose the best option, which was SE-GLCM-MLR.

As for the research of Caballero *et al.* (2017b) with fractal algorithms, there were also found significant differences in all fractal features among GE, SE and T3D acquisition sequences. The prediction results were affected by the sequence acquisition, the fractal algorithm and the data mining technique, finding the best prediction results with the combination SE-OPFTA-MLR. In fact, SE offers a better performance in terms of signal to noise ratio than GE and T3D, OPFTA simulates the texture of the MRI better than FTA and CFA (Caballero *et al.*, 2018), and MLR is recommended when the values of the database are not highly correlated (Pérez-Palacios *et al.*, 2014).

In the 3D study of Ávila *et al.* (2018), the MRI analysis initiated with the selection of a ROI of 20 x 20 pixels. The ROIs of all the images of a piece were reconstructed in three dimensions by linear interpolation methods. Then, the 3D reconstructed MRI of loins were analysed by the three classical algorithms for texture analysis adapted to work with three-dimensional images. Again, the influence

of the sequence acquisition on the values of the computational texture features was detected. As occurred in the study of Perez-Palacios *et al.* (2017) with two-dimensional images, combinations of SE or GE with any texture algorithm and any regression technique offered precise prediction results for the physico-chemical parameters of loins. However, Ávila *et al.* (2018), taking into consideration the computational cost apart from the accuracy of the methodology, proposed the combination of GE-3D GLCM-IR as the best option.

In these studies, to validate the optimum procedure achieved, the adjustment between real and predicted values of the physico-chemical parameters analysed were statistically compared, having both groups of data the same performance and not being significantly different.

Another recent study on pork loins has been published by Ávila *et al.* (2019), who used a LF-H[1] MRI scanner with a hand/wrist coil and SE T1-weighted acquisition sequences to predict physico-chemical characteristics of fresh loins. The authors of this study considered that conclusions of the previous works at evaluating the use of MRI to analyse meat might be preliminary, due to the use of conventional texture descriptors and regressors instead of stronger methods and of optimistic methodology to measure the performance. In this sense, experiments of this study were developed with 15 texture descriptors to analyse the MRI (such as Haralick descriptors, local binary patterns, fractal features, Gabor or wavelet features), in combination to 28 regression techniques to analyse the data (linear regressors, neural networks, deep learning, support vector machines, regression trees, ensembles, boosting machines and random forests, among others), having 720 combinations in total. To guarantee a realistic evaluation, three data partitions (for training, validation and test) were used instead of the usual two sets (training and test sets), and the dataset was created leaving one meat piece out, instead of the common random partitioning of the image collection. The test set was composed by one meat piece, while the images of the remaining meat pieces were divided into the training and validation sets at random. Good to excellent prediction results were achieved for most physico-chemical parameters analysed, but there was not possible to set a common combination of texture vector and regressor that provides accurate correlations for all characteristics tested.

Most recent studies on MRI and fresh meat have been focused on analysing the effect of freezing/thawing. Cheng *et al.* (2019) worked with beef *semimembranosus* muscles that were scanned by using a LF-H[1] and SE acquisition sequences weighted in T1 and T2. The image analysis of this study consists of measuring the relative intensity of the MRI from samples subjected to 0, 1, 2, 3, 4, 5, 6, 7 freeze-thaw cycles. The obtained data were analysed by ANOVA followed by the Tukey procedure. The signal intensity of T1 and T2 images significantly decreased as the number freeze-

thaw cycles increased. Besides, it was observed a decrease in the brighter of the T1 and T2 images from external to centre regions with the increase of the freeze-thaw cycles.

The assessment of the loss of quality of chicken breast due to freezing/thawing was study by Frelka *et al.* (2019), who used a HF-H^1 MRI with a knee coil. Three different sequences acquisition were tested (3D T1 – rapid GE, proton density – turbo SE and T2 – turbo SE). The analysis of the images was done visually and by measuring the percentage of pixels. The water changes that take place during the freezing/thawing cycles were clearly observed in the images from the three sequence acquisitions. The quantitative analyses based on the percentage of pixels were only done in the images from proton density and T2 sequences, noting differences between unfrozen and frozen/thawed samples, especially in proton density images.

6. ADVANTAGES AND DISADVANTAGES OF NON-DESTRUCTIVE TECHNIQUES METHODS

Some of the greatest advantages of NIRs in meat quality evaluation are that it is non-destructive, can be non-contact, and has varying degrees of portability to meet different application needs. The typical halogen light source is easily available, and technological advances are ever increasing compactness, ruggedness, and accuracy, as well as decreasing cost. The technology also has a number disadvantages particularly related to the inhomogeneity and high moisture content of meat. The former requires that intact samples have large or multiple reading areas, and the latter that both sample and ambient temperature remain consistent. Additionally, in an industrial situation where NIRs could be used for monitoring or sorting on a moving belt, samples are not static, due to shape variations the distance from a fixed reading head is inconsistent, and data collection and analysis must be rapid. As discussed above, there has been some progress in several of these areas and the future looks promising.

The main advantage of HSI technology is the ability in predicting the concentration gradient of chemical constituents as spatial distribution, which can be especially useful for visualizing meat quality traits. HSI allows to merge the digital imaging spatial resolution with the chemical information obtainable by point spectroscopy. This is particularly relevant for fat content and distribution modelling, indeed the success in intramuscular fat determination could permit producers to exploit to the maximum level the quality of each meat cut answering the specific needs of the market.

The huge disadvantage of HSI technology is related to the long acquisition time and the large amount of produced data for each single measure. However, simplified instruments (multiband cameras) developed for specific applications could reduce the spectral range to be scanned up to few selected

wavelength, thus minimizing both acquisition time and generated data, which anyway will be fast managed with the proper *ad hoc* chemometric method.

One of the benefits of using NMR is the high sensitivity for distinguishing the different component of the meat, which is due to the strength of the magnetic field and it is dependent on the presence of the magnetic atom on the sample to analyze. Thus, the evaluation of fresh meat, which has a high content of ^{1}H, by NMR with antennas for exciting ^{1}H spin, achieves accurate results. It is also notable, the low time of analysis of NMR systems, being lower than 2 minutes per sample. However, this technique is quite sensitive to changes of the temperatures, being necessary low room-temperature to have accurate results. In addition, the size of the samples to be analyse should be very small, which require their destruction in some cases.

The use of MRI-computer vision as an alternative methodology to analyse different quality parameters of meat offers the advantage of being a non-destructive, non-invasive, non-radiant and innocuous techniques. Besides, it takes less time than traditional and destructive methods. However, some improvements, mainly on the image acquisition time and software, should be developed in order to work automatically, give the results on-line and fulfil the requirements of the meat industries. This is the only technique be able to take information from the inner of solid samples of medium-large volume, and consequently, it is really interesting for meat pieces such as loins or hams.

CONCLUSIONS AND FURTHER STUDIES.

The use of NIRs in the laboratory for objective assessment of meat quality is developing, with best results for composition-related measurements. Colour, pH, and drip loss are predicted best when the VIS-NIRs spectra is used. Routine use of NIRs on a production line is still in the future, although possibly a very near future. Technological advances reducing size, cost, and data analysis time are making NIRs more easily available, although new equipment should not be blindly used, but tested for accuracy and precision before being relied upon.

Most of the reported works are feasibility studies mainly developed at laboratory scale, whereas there is a lack of studies proving model's robustness at processing plant level. Thus, more effort is desired to bridge the gap between spectroscopic devices' potential and their implementation as Process Analytical Technology tool, and this way should involve both researchers and industries. Furthermore, few cases present a data fusion approach, which could be considered a strategic way to improve quality attribute prediction by non-destructive techniques. For instance, the combination of HSI and digital image analysis could provide improved models for quality assessment at industrial level.

NMR systems noted for their high sensitivity and accurate in the detection of the component of the meat and for the analysis speed. The most studies developed with NMR on fresh meat have been carried out with LF-NMR systems, with CPMG as pulse sequence and T2 as relaxation time. The results obtained show the ability of this technique to determine main physico-chemical parameters of fresh meat, and to evaluate the effects of cooking and freezing/thawing.

In the last decade, most studies developed with MRI on fresh meat have been carried with low-field scanners, to optimize the methodology and predict quality parameters of loins. Nevertheless, the use of high-field scanners has been reduced in the last years, being mainly applied with classification purposes. The latest publications on MRI have been focused on evaluating of the effect of freezing/thawing on meat. The accurate results obtained on these MRI studies allow you to indicate that the combination of different acquisition parameters, algorithms for analysing the images and data analysis techniques can be proposed as an alternative methodology to analyse fresh meat with high reliability in a non-destructive way. Nevertheless, the future work will be to operate as a quality assessment system in the meat industries, by improving the time for image acquisition and to develop a software that analyses the images automatically and provides the results on-line.

ACKNOWLEDGMENTS

Daniel Caballero thanks the “Junta de Extremadura” for the post-doctoral grant (PO17017). The authors wish to acknowledge the funding received from the “Junta de Extremadura” (Regional Government Board. Research Project (IB16089)).

REFERENCES

Abbott, J. A. (1999). Quality measurement of fruits and vegetables. *Postharvest Biology and Technology*, 15, 207–225.

Alander, J. T., Bochko, V., Martinkauppi, B., Saranwong, S. & Mantere, T. (2013) A review of optical nondestructive visual and near infra-red methods for food quality and safety. *International Journal of Spectroscopy*. Article ID 341402.

Amigo, J. M. (2020). Hyperspectral and multispectral imaging: setting the scene. In Amigo, J. M. (Eds.), *Hyperspectral Imaging* (pp. 3-16). Amsterdam: Elsevier Science.

Amigo, J. M., & Grassi, S. (2020). Configuration of hyperspectral and multispectral imaging systems. In Amigo, J. M. (Eds.), *Hyperspectral Imaging* (pp. 17-34). Amsterdam: Elsevier Science.

Andersen, P. V., Veiseth-Kent, E. & Wold, J. P. (2017). Analyzing pH-induced changes in a myofibril model system with vibrational and fluorescence spectroscopy. *Meat Science*, 125, 1-9.

Andersen, P. V., Wold, J. P., Gjerlaug-Enger, E. & Veiseth-Kent, E. (2018a). Predicting post-mortem meat quality in porcine longissimus lumborum using Raman, near infrared and fluorescence spectroscopy. *Meat Science*, 145, 94-100.

Andersen, P. V., Wold, J. P., & Veiseth-Kent, E. (2018b). Analyzing μ-Calpain induced proteolysis in a myofibril model system with vibrational and fluorescence spectroscopy. *Meat Science*, 139, 239-246.

Ávila, M. M., Caballero, D., Durán, M. L., Caro, A., Pérez-Palacios, T., & Antequera, T. (2015). Including 3D-textures in a Computer Vision System to analyze quality traits of loin. *Lecture Notes in Computer Science*, 9163, 456-465.

Ávila, M. M., Caballero, D., Antequera, T., Durán, M. L., Caro, A., & Pérez-Palacios, T. (2018). Applying 3D textures algorithms on MRI to evaluate quality traits of loin. *Journal of Food Engineering*, 222, 258-266.

Ávila, M. M., Durán, M. L., Caballero, D., Antequera, T., Pérez-Palacios, T., Cernadas, E., & Fernández-Delgado, M. (2019). Magnetic Resonance Imaging, texture analysis and regression techniques to non-destructively predict the quality characteristics of meat pieces. *Engineering Applications of Artificial Intelligence*, 82, 110-125.

Bajd, F., Škrlep, M., Čandek-Potokar, M., & Serša, I. (2017). MRI-aided texture analysis of compressed meat products. *Journal of Food Engineering*, 207, 108-118.

Barbin D. F., Elmasry G., Sun D. W., & Allen P. (2012). Predicting quality and sensory attributes of pork using near-infrared hyperspectral imaging. *Analytica Chimica Acta*, 719, 30–42.

Barbin, D. F., ElMasry, G., Sun, D. W., & Allen, P. (2013). Non-destructive determination of chemical composition in intact and minced pork using near-infrared hyperspectral imaging. *Food Chemistry*, 138, 1162-1171.

Barlow, R. E., Bartholomew, D., Bremner, J. M., & Brunk, H. D. (1972). *Statistical inference under order restriction: the theory and application of isotonic regression.* New York, New York, U.S.A.: Ed. Wiley.

Bernau, M., Kremer, P. V., Lauterbach, E., Tholen, E., Petersen, B., Pappenberger, E., & Scholz, A. M. (2015). Evaluation of carcass composition of intact boars using linear measurements from performance testing, dissection, dual energy x-ray absorptiometry (DXA) and magnetic resonance imaging (MRI). *Meat Science*, 104, 58-66.

Bertram, H. C., Aaslyng, M. D., & Andersen, H. J. (2005). Elucidation of the relationship between cooking temperature, water distribution and sensory attributes of pork – a combined NMR and sensory study. *Meat Science*, 70, 75-81.

Bro, R. (1996). Multiway calibration. Multilinear PLS. *Journal of Chemometrics*,10, 47-61.

Bro, R. & Smilde, A. K. (2014). Principal Component Analysis. *Analytical Methods*, 6, 2812-2831.

Caballero, D., Caro, A., Rodríguez, P. G., Durán, M. L., Ávila, M. M., Palacios, R., . . . Pérez-Palacios, T. (2016). Modeling salt diffusion in Iberian ham by applying MRI and data mining. *Journal of Food Engineering*, 189, 115-122.

Caballero, D., Pérez-Palacios, T., Caro, A., Amigo, J. M., Dahl, A. B., Ersboll, B. K., & Antequera, T. (2017a). Prediction of pork quality parameters by applying fractals and data mining on MRI. *Food Research International*, 99, 739-747.

Caballero, D., Caro, A., Ávila, M. M., Rodríguez, P. G., Antequera, T., & Pérez-Palacios, T. (2017b). New fractal features and data mining to determine food quality based on MRI. *IEEE on Latin American Transactions*, 15(9), 1777-1784.

Caballero, D., Caro, A., Dahl, A. B., Ersboll, B. K., Amigo, J. M., Pérez-Palacios, T., & Antequera, T. (2018). Comparison of different image analysis algorithms on MRI to predict physico-chemical and sensory attributes of loin. *Chemometrics and Intelligent Laboratory Systems*, 180, 54-63.

Caro, A., Rodríguez, P. G., Cernadas, E., Durán, M. L., & Villa, D. (2001). Applying active contours to muscle recognition in Iberian ham MRI. In: *IASTED International Conference on Signal Processing, Pattern Recognition and Applications*. Rhodes, Greece.

Caro, A., Rodríguez, P. G., Durán, M. L., & Antequera, T. (2012). Active contours for real time applications. In: Flournier, M. D. (ed.). *Perspective on Pattern Recognition.* Hauppauge, New York, U. S. A.: Nova Science Publishers Inc. (pp. 173-186).

Cheng, W., Sun, D. W., Pu, H., & Liu, Y. (2016). Integration of spectral and textural data for enhancing hyperspectral prediction of K value in pork meat. *LWT-Food Science and Technology*, 72, 322-329.

Cheng, S., Wang, X., Li, R., Yang, H., Wang, H., Wang, H, & Tana, M. (2019). Influence of multiple freeze-thaw cycles on quality characteristics of beef Semimembranosus muscle: With emphasis on water status and distribution by LF-NMR and MRI. *Meat Science*, 147, 44–52.

Cheriet, M., Said, J. N., & Suen, C. Y. (1998). A recursive thresholding technique for image segmentation. *IEEE Transactions on Image Processing*, 7(6), 918-921.

Cortés, V., Blasco, J., Aleixos, N., Cubero, S. & Talens, P. (2019) Monitoring strategies for quality control of agricultural products using visible and near-infrared spectroscopy: a review. *Trends in Food Science & Technology*. 85:138-148.

Craig, A. Cloarec, O., Holmes, E., Nicholson, J. K., & Lindon, J. C. (2006). Scaling and normalization effects in NMR spectroscopic metabonomic data sets. *Analytical Chemistry*, 78, 2262-2267.

Craigie, C. R., Johnson, P. L., Shorten, P. R., Charteris, A., Maclennan, G., Tate, M. L., ... & Reis, M. M. (2017). Application of Hyperspectral imaging to predict the pH, intramuscular fatty acid content and composition of lamb M. longissimus lumborum at 24 h post mortem. *Meat Science*, 132, 19-28.

Delorme, A., Sejnowski, T., & Makeig, S. (2007). Enhanced detection of artifacts in EEG data using higher-order statistics and independent component analysis. *Neuroimage*, 34(4), 1443-1449.

Dixit, Y., Casado-Gavalda, M. P., Cama-Moncunill, R., Cama-Moncunill, X., Cullen, P. J., & Sullivan, C. (2016a). Prediction of beef fat content simultaneously under static and motion conditions using near infrared spectroscopy. *Journal of Near Infrared Spectroscopy*, 24(4), 353-361.

Dixit, Y., Casado-Gavalda, M. P., Cama-Moncunill, R., Cama-Moncunill, X., Jacoby, F., Cullen, P. J., & Sullivan, C. (2016b). Multipoint NIR spectrometry and collimated light for predicting the composition of meat samples with high standoff distances. *Journal of Food Engineering*, 175, 58-64.

Dixit, Y., Casado-Gavalda, M. P., Cama-Moncunill, R., Markiewicz-Keszycka, M., Cruise, P., Jacoby, F., . . . Sullivan, C. (2016c). NIR spectrophotometry with integrated beam splitter as a process analytical technology for meat composition analysis. *Analytical Methods*, 8(20), 4134-4141.

Dixit, Y., Casado-Gavalda, M. P., Cama-Moncunill, R., Cama-Moncunill, X., Markiewicz-Keszycka, M., Cullen, P. J., & Sullivan, C. (2017). Developments and challenges in online NIR spectroscopy for meat processing. *Comprehensive Reviews in Food Science and Food Safety*, 16(6), 1172-1187.

ElMasry, G., & Sun, D. W. (2010). Principles of Hyperspectral Imaging Technology. In *Hyperspectral Imaging Food Qual. Anal. Control*, 3-43.

ElMasry, G., Sun D. W., & Allen P. (2011). Non-destructive determination of water-holding capacity in fresh beef by using NIR hyperspectral imaging. *Food Research International*, 44, 2624–2633.

ElMasry, G., Sun, D. W., & Allen, P. (2013). Chemical-free assessment and mapping of major constituents in beef using hyperspectral imaging. *Journal of Food Engineering*, 117, 235-246.

ElMasry, G., Mandour, N., Al-Rejaie, S., Belin, E., & Rousseau, D. (2019). Recent applications of multispectral imaging in seed phenotyping and quality monitoring—An overview. *Sensors*, 19, 1090.

Fayyad, U., Piatetsky-Shapiro, G., & Smyth, P. (1996). From data mining to knowledge discovery in databases. *American Association for Artificial Intelligence*, 17, 37-54.

Feig, S. (2011). Comparison of costs and benefits of breast cancer screening with Mammography, Ultrasonography, and MRI. *Obstetrics and Gynecology Clinics of North America*, 38(1),

Frelka, J. C., Phinney, D. M., Yang, X., Knopp, M. V., Heldman, D. R., Wick, M. P., & Vodovotza, Y. (2019). Assessment of chicken breast meat quality after freeze/thaw abuse using magnetic resonance imaging techniques. *Journal of the Science of Food and Agricultural*, 99, 844–853.

Gentilin, F. A., Kobo, B. T., De Souza Ribeiro, L., De França, J. A., De Felício, A. L. S. M., De França, M. B., & De O Toginho Filho, D. (2016). Development and testing of a hardware platform for measuring instruments based on near-infrared diffuse reflection. Measurement: *Journal of the International Measurement Confederation*, 86, 14-25.

Gottschall, T., Meyer, T., Schmitt, M., Popp, J., Limpert, J., & Tünnermann, A. (2018). Advances in laser concepts for multiplex, coherent Raman scattering micro-spectroscopy and imaging, *TrAC - Trends Analytical Chemistry*, 102, 103–109.

Guo, T., Huang, M., Zhu, Q., Guo, Y., & Qin, J. (2018). Hyperspectral image-based multi-feature integration for TVB-N measurement in pork. *Journal of Food Engineering*, 218, 61-68.

Habib, M., & Ullah, A. (2016). Simulation of near infrared interference bandpass filters for spectroscopic applications. Paper presented at the 1st International Conference on Computing, Electronic and Electrical Engineering, ICE Cube 2016.

Harrington, P. d. B. (2018). Feature expansion by a continuous restricted Boltzmann machine for near-infrared spectrometric calibration. *Analytica Chimica Acta*, 20, 20-28.

Hansen, C. L., Van Der Berg, F., Ringgard, S., Stødkilde-Jørgensen, H., & Karlsson, A. H. (2008). Diffusion of NaCl in meat studied by ^{1}H and ^{23}Na magnetic resonance imaging (MRI). *Journal of Food Engineering*, 31, 457-471.

Hastie, T., Tibshirani, R., & Friedman, J. (2001). *The elements of statistical learning: data mining inference and prediction*. New York, New York, U.S.A.: Ed. Springer-Verlag.

Hendrick, R. E. (2005). *Glossary of MR Terms.* 5th ed. Reston, Virginia, U.S.A.: American College of Radiology.

Hibbert, D. B. (1991). Fractals in chemistry. *Chemometrics and Intelligent Laboratory Systems*, 11, 1-11.

Hornak, J. P. (1997). *The basics of NMR.* Rochester, New York, U.S.A.: Rochester Institute of Technology.

Huang, H., Liu, L., & Ngadi, M. O. (2017). Assessment of intramuscular fat content of pork using NIR hyperspectral images of rib end. *Journal of Food Engineering*, 193, 29-41.

Ishikawa, D., Ueno, G., & Fujii, T. (2017). Estimation method of moisture content at the meat surface during drying process by NIR spectroscopy and its application for monitoring of water activity. *Japan Journal of Food Engineering*, 18(3), 135-143.

Jakes, W., Gerdova, A., Defernez, M., Watson, A. D., McCallum, C., Limer, E., . . . Kemsley, E. K. (2015). Authentication of beef versus horse meat using 60 MHz 1 H NMR spectroscopy. *Food Chemistry*, 175, 1-9.

Jia, G., Liu, H., Nirasawa, S., & Liu, H. (2017). Effects of high-voltage electrostatic field treatment on the thawing rate and post-thawing quality of frozen rabbit meat. *Innovative Food Science and Emerging Technologies*, 41, 348-356.

Kademi, H. I., Ulusoy, B. H., & Hecer, C. (2019). Applications of miniaturized and portable near infrared spectroscopy (NIRS) for inspection and control of meat and meat products. *Food Reviews International*, 35(3), 201-220.

Kamruzzaman, M., ElMasry, G., Sun, D. W., & Allen, P. (2012a). Non-destructive prediction and visualization of chemical composition in lamb meat using NIR hyperspectral imaging and multivariate regression. *Innovative Food Science & Emerging Technologies*, 16, 218–26.

Kamruzzaman, M., ElMasry, G., Sun, D. W., & Allen, P. (2012b). Prediction of some quality attributes of lamb meat using near-infrared hyperspectral imaging and multivariate analysis. *Analytica Chimica Acta*, 714, 57-67.

Kamruzzaman, M., Makino, Y., & Oshita, S. (2015). Non-invasive analytical technology for the detection of contamination, adulteration, and authenticity of meat, poultry, and fish: a review. *Analytica Chimica Acta*, 853, 19-29.

Kamruzzaman, M., Makino, Y., & Oshita, S. (2016a). Online monitoring of red meat color using hyperspectral imaging. *Meat Science*, 116, 110-117.

Kamruzzaman M., Makino, Y., & Oshita S. (2016b). Hyperspectral imaging for real-time monitoring of water holding capacity in red meat. *LWT-Food Science and Technology*, 66, 685–691.

Kandpal, L., Lee, H., Kim, M., Mo, C., & Cho, B. K. (2013). Hyperspectral reflectance imaging technique for visualization of moisture distribution in cooked chicken breast. *Sensors*, 13, 13289-13300.

Kandpal, L. M., Lee, J., Bae, J. Lohumi, S. & Cho, B. K. (2019) Development of a low-cost multi-waveband LED illumination imaging technique for rapid evaluation of fresh meat quality. *Applied Sciences*, 9, Article 912.

Khulal, U., Zhao, J., Hu, W., & Chen, Q. (2017). Intelligent evaluation of total volatile basic nitrogen (TVB-N) content in chicken meat by an improved multiple level data fusion model. *Sensors and Actuators B: Chemical*, 238, 337-345.

Knight, M. I., Linden, N., Ponnampalam, E. N., Kerr, M. G., Brown, W. G., Hopkins, D. L., . . . Wesley, I. (2019). Development of VISNIR predictive regression models for ultimate pH, meat tenderness (shear force) and intramuscular fat content of Australian lamb. *Meat Science*, 155, 102-108.

Kobayashi, K. I., Matsui, Y., Maebuchi, Y., Toyota, T., & Nakauchi, S. (2010). Near infrared spectroscopy and hyperspectral imaging for prediction and visualisation of fat and fatty acid content in intact raw beef cuts. *Journal of Near Infrared Spectroscopy*, 18, 301-315.

Kobayashi, K. I., Mori, M., Nishino, K., Toyota, T., & Nakauchi, S. (2012). Visualisation of fat and fatty acid distribution in beef using a set of filters based on near infrared spectroscopy. *Journal of Near Infrared Spectroscopy*, 20, 509-519.

Kohavi, R., 1995. A study of cross-validation and bootstrap for accuracy estimation and model selection. In: International Joint Conference on Artificial Intelligence IJCAI, Montréal, Canada, pp. 1137–1143.

Konarska, M., Kuchida, K., Tarr, G., & Polkinghorne, R. J. (2017). Relationships between marbling measures across principal muscles. *Meat Science*, 123, 67-78.

Lee, H., Kim, M. S., Lee, W. H., & Cho, B. K. (2018). Determination of the total volatile basic nitrogen (TVB-N) content in pork meat using hyperspectral fluorescence imaging. *Sensors and Actuators B: Chemical*, 259, 532-539.

Lee, S., Lohumi, S., Lim, H. S., Gotoh, T., Cho, B. K., & Jung, S. (2015). Determination of intramuscular fat content in beef using magnetic resonance imaging. *Journal of the Faculty of Agriculture from Kyushu University*, 60(1), 157-162.

Li, H., Chen, Q., Zhao, J., & Wu, M. (2015). Nondestructive detection of total volatile basic nitrogen (TVB-N) content in pork meat by integrating hyperspectral imaging and colorimetric sensor combined with a nonlinear data fusion. *LWT-Food Science and Technology*, 63, 268-274.

Li, W., Wang, P., Xu, X., Xing, T., & Zhou, G. (2014). Use of low-field nuclear magnetic resonance to characterize water properties in frozen chicken breasts thawed under high pressure. *European Food Research and Technology*, 239, 183-188.

Li, X., Feng, F., Gao, R., Wang, L., Qian, Y., Li, C., & Zhou, G. (2016). Application of near infrared reflectance (NIR) spectroscopy to identify potential PSE meat. *Journal of the Science of Food and Agriculture*, 96(9), 3148-3156.

Li, Z., Jia, C., Wang, X., Liu, Q., & Dong, C. (2016). Nondestructive determination of beef textural properties by near infrared spectroscopy. *Nongye Gongcheng Xuebao/Transactions of the Chinese Society of Agricultural Engineering*, 32(16), 286-292.

Liu, C., Pan, D., Ye, Y., & Cao, J. (2013). ^{1}H NMR and multivariate data analysis of the relationship between the age and quality of duck meat. *Food Chemistry*, 141, 1281-1286.

Liu, L. and Ngadi, M. O. (2014). Predicting intramuscular fat content of pork using hyperspectral imaging. *Journal of Food Engineering*, 134, 16–23.

Lohumi, S., Lee, S., Lee, H., Kim, M. S., Lee, W. H. and Cho, B. K. (2016). Application of hyperspectral imaging for characterization of intramuscular fat distribution in beef. *Infrared Physics and Technology*, 74, 1–10.

Maravall, D. (1993). *Reconocimiento de formas y Visión Artificial*. Madrid, Spain: Ed. Ra-ma.

Martens, H., & Naes, T. (1989). *Multivariate Calibration*. New York, New York, U.S.A.: Ed. Wiley.

McIntosh, P. (2013). CPMG. In: Roberts G. C. K. (ed). *Encyclopedia of Biophysics* (pp. 386). Berlin, Germany: Ed. Springer.

Mínguez, C., Sánchez, J. P., Hernández, P., Ragab, M., El Nagar, A. G., & Baselga, M. (2017). Genetic analysis of meat quality traits in maternal lines of rabbit and their diallel cross. *Meat Science*, 131, 1-8.

Mobaraki, N., & Amigo, J. M. (2018). HYPER-Tools. A graphical user-friendly interface for hyperspectral image analysis. *Chemometrics and Intelligent Laboratory Systems*, 172, 174-187.

Molano, R., Rodríguez, P. G., Caro, A., & Durán, M. L. (2012). Finding the largest area rectangle of arbitrary orientation in a closed contour. *Applied Mathematics and Computation*, 218, 9866-9874.

Moran, L., Andres, S., Allen, P., & Moloney, A. (2018). Visible and near infrared spectroscopy as an authentication tool: Preliminary investigation of the prediction of the ageing time of beef steaks. *Meat Science*, 142, 52- 58.

Nolasco-Perez, I. M., Rocco, L. A. C. M., Cruz-Tirado, J. P., Pollonio, M. A. R., Barbon, S., Barbon, A. P. A. C., & Barbin, D. F. (2019). Comparison of rapid techniques for classification of ground meat. *Biosystems Engineering*, 183, 151-159.

Otsu, N. (1979). A threshold selection method from gray-level histograms. *IEEE Transactions on Systems, Man, and Cybernetics*, 9(1), 62-66.

Pasquini, C. (2018). Near infrared spectroscopy: A mature analytical technique with new perspectives - a review. *Analytica Chimica Acta*, 1026, 8-36.

Pereira, F. M. V., & Colnago, L. A. (2012). Determination of the moisture content in Beef without weighing benchtop time-domain nuclear magnetic resonance spectrometer and chemometrics. *Food Analytical Methods*, 5, 1349-1353.

Pérez-Palacios, T., Antequera, T., Durán, M. L., Caro, A., Rodríguez, P. G., & Palacios, R. (2011). MRI-based analysis of feeding background effect on fresh Iberian ham. *Food Chemistry,* 126, 1366-1372.

Pérez-Palacios, T., Caballero, D., Caro, A., Rodríguez, P. G., & Antequera, T. (2014). Applying data mining and computer vision techniques to MRI to estimate quality traits in Iberian hams. *Journal of Food Engineering*, 131, 82-88.

Pérez-Palacios, T., Caballero, D., Antequera, T., Durán, M. L., Ávila, M. M., & Caro, A. (2017). Optimization of MRI acquisition and texture analysis to predict physico-chemical parameters of loins by data mining. *Food and Bioprocess Technology*, 10, 750-758.

Perez-Palacios, T., Caballero, D., González-Mohíno, A., Mir-Bel, J., & Antequera T. (2019). Near Infrared Reflectance spectroscopy to analyse texture related characteristics of sous vide pork loin. *Journal of Food Engineering*, 263, 417-423.

Piao, S., Okura, T., & Irie, M. (2018). On-site evaluation of Wagyu beef carcasses based on the monounsaturated, oleic, and saturated fatty acid composition using a handheld fiber-optic near-infrared spectrometer. *Meat Science*, 137, 258-264.

Pieszczek, L., Czarnik-Matusewicz, H., & Daszykowski, M. (2018). Identification of ground meat species using near-infrared spectroscopy and class modeling techniques – Aspects of optimization and validation using a one-class classification model. *Meat Science*, 139, 15-24.

Poerio, D. V., & Brown, S. D. (2017). Stacked interval sparse partial least squares regression analysis. *Chemometrics and Intelligent Laboratory Systems*, 166, 49-60.

Prevolnik Povsě, M., Karolyi, D., Tomažin, U., Škrlep, M., Pugliese, C., Lebret, B., & Čandek-Potokar, M. (2017). Accuracy of near infrared spectroscopy to predict quality of pork and pork products including samples of Krškopolje and Turopolje pigs. *Agriculturae Conspectus Scientificus*, 82(3 Special Issue 2), 205-209.

Prieto, N., Pawluczyk, O., Dugan, M. E. R., & Aalhus, J. L. (2017). A review of the principles and applications of near-infrared spectroscopy to characterize meat, fat, and meat products. *Applied Spectroscopy*, 71(7), 1403-1426.

Prieto, N., Osika, E., Aalhus, J. L., Lopez-Campos, O., Juarez, M., & Pawluczyk, O. (2018). Application of hyperspectral imaging on meat and meat products. *CAB Reviews*, 13, 1-11.

Pu, H., Sun, D. W., Ma, J., Liu, D., & Kamruzzaman, M. (2014). Hierarchical variable selection for predicting chemical constituents in lamb meats using hyperspectral imaging. *Journal of Food Engineering*, 143, 44-52.

Qin, J., (2010). Hyperspectral Imaging Instruments. In: Sun, D. W. (Eds.), *Hyperspectral Imaging for Food Quality Analysis and Control* (pp. 129–172). Amsterdam: Academic Press.

Qu, F., Ren, D., He, Y., Nie, P., Lin, L., Cai, C., & Dong, T. (2018). Predicting pork freshness using multi-index statistical information fusion method based on near infrared spectroscopy. *Meat Science*, 146, 59-67.

Rady, A., & Adedeji, A. (2018) Assessing different processed meats for adulterants using visible-near-infrared spectroscopy. *Meat Science*, 136:59-67.

Raof, R. A. A., Salleh, Z., Sahidan, M. Y., Mashor, S. S., Noor, M., Mohamad, I. F., & Hasan, H. (2008). Color thresholding method for image segmentation algorithm of Ziehl-Neelsen sputum slide images. *Lecture Notes in Electrical Engineering*, 367, 212-217.

Reis, M. M., Van Beers, R., Al-Sarayreh, M., Shorten, P., Yan, W. Q., Saeys, W., ...& Craigie, C. (2018). Chemometrics and hyperspectral imaging applied to assessment of chemical, textural and structural characteristics of meat. *Meat Science*, 144, 100-109.

Richli, M. M., Kaufmann, D., & Scheeder, M. (2016). Prediction of the fatty acid composition in backfat of pigs as breeding tool. *Agrarforschung Schweiz*, 7(4), 180-187.

Rinnan, A., Van der Berg, F., & Engelsen S. B. (2009). Review of most common pre-processing techniques for near-infrared spectra. *Trends in Analytical Chemistry*, 28, 1201-1222.

Ripoll, G., Lobón, S., & Joy, M. (2018). Use of visible and near infrared reflectance spectra to predict lipid peroxidation of light lamb meat and discriminate dam's feeding systems. *Meat Science*, 143, 24-29.

Savitzky, A., & Golay, M. J. E. (1964). Smoothing and differentiation of data by simplified least squares procedures. *Analytical Chemistry*, 36(8), 1627-1639.

Savorani, F., Tomasi, G., & Engelsen, S. B. (2010). Icoshift: a versatile tool for the rapid alignment of 1D NMR spectra. *Journal of Magnetic Resonance*, 202, 190-202.

Shaarani, S. M., Nott, K. P., & Hall, L. D. (2006). Combination of NMR and MRI quantification of moisture and structure changes for convection cooking of fresh chicken meat. *Meat Science*, 72, 398-403.

Soladoye, O. P., Prieto, N., Lopez-Campos, O., Aalhus, J. L., Uttaro, B., Roberts, J. C., . . . Juárez, M. (2018). Potential of near infrared (NIR) spectroscopy and dual energy X-ray absorptiometry (DXA) in predicting pork belly softness. *Meat Science*, 142, 1-4.

Sonka, M., Hlavac, V., & Boyle, R. (1999). *Image processing, analysis, and machine vision.* Pacific Grove, California, U.S.A.: Ed. PWS Publishing.

Straadt, I. K., Rasmussen, M., Andersen, H. J., & Bertram, H. C. (2006). Aging-induced changes in microstructure and water distribution in fresh and cooked pork in relation to water-holding capacity and cooking loss – a combined confocal laser scanning microscopy (CLSM) and low-field nuclear magnetic resonance relaxometry study. *Meat Science*, 75, 687-695.

Ullah, A., Butt, M. A., Fomchenkov, S. A., & Khonina, S. N. (2016). Indium phosphide all air-gap Fabry-Pérot filters for near-infrared spectroscopic applications. Paper presented at the 3rd International School and Conference on Optoelectronics, Photonics, Engineering and Nanostructures, Saint Petersburg OPEN 2016.

Vala, H. J., & Baxi, A. (2013). A review on Otsu image segmentation algorithm. *International Journal of Advanced Research in Computer Engineering & Technology*, 2(2), 387-389.

Venturi, L., Rocculi, P., Cavani, C., Placucci, G., Dalla Rosa, M., & Cremonini, M. A. (2007). Water absorption of freeze-dried meat at different water activities: a multi-analytical approach using sorption isotherm, differential scanning calorimetric and nuclear magnetic resonance. *Journal of Agricultural and Food Chemistry*, 55, 10572-10578.

Vestergaard, C., Risum, J., & Adler-Nissen, J. (2005). ^{23}Na-MRI quantification of sodium and water mobility in pork during brine curing. *Meat Science,* 69, 663-672.

Vidal, M., & Amigo, J. M. (2012). Pre-processing of hyperspectral images. Essential steps before image analysis. *Chemometrics and Intelligent Laboratory Systems*, 117, 138-148.

Wang, H., Tian, H. Y., Zhang, S. L., Zhang, H., Zhao, B., Li, J. P., & Qiao, X. L. (2017). On-line noninvasive prediction of cholesterol level of fresh pork within NIR medium wavelength region with portable near-infrared spectrometer. *Guang Pu Xue Yu Guang Pu Fen Xi/Spectroscopy and Spectral Analysis*, 37(6), 1759-1764.

Wang, W., Peng, Y., Zheng, X., Tian, F., & Wei, W. (2016). A non-destructive detection system for determination of multi-quality parameters of meat. Paper presented at the 2016 ASABE Annual International Meeting.

Wang, W., Peng, Y., Sun, H., & Li, L. (2017). Real-time detection of intact pork freshness based on near infrared spectroscopy. Paper presented at the 2017 ASABE Annual International Meeting.

Wang, W., Peng, Y., Sun, H., Wei, W., & Zheng, X. (2018a). Evaluation of pork freshness using two-dimensional correlation visible/near-infrared spectroscopy combined with support vector machine. *Shipin Kexue / Food Science*, 39(18), 273-279.

Wang, W., Peng, Y., Sun, H., Zheng, X., & Wei, W. (2018b). Real-time inspection of pork quality attributes using dual-band spectroscopy. *Journal of Food Engineering*, 237, 103-109.

Weisskopf, V. F. (2010). How Light Interacts with Matter. *Scientific American*, 219, 60–71.

Williams, P. & Norris, K. (Eds.) (2004) *Near-Infrared Technology in the Agricultural and Food Industries*. 2nd Ed. American Association of Cereal Chemists, Inc., St. Paul, MN, USA.

Wold, J. P., O'Farrell, M., Høy, M. & Tschudi, J. (2011). On-line determination and control of fat content in batches of beef trimmings by NIR imaging spectroscopy. *Meat Science*, 89, 317–324.

Wu, J., Peng, Y., Li, Y., Wang, W., Chen, J., & Dhakal, S. (2012). Prediction of beef quality attributes using VIS/NIR hyperspectral scattering imaging technique. *Journal of Food Engineering*, 109, 267–73.

Wu, T., Zhong, N., & Yang, L. (2018). Application of VIS/NIR spectroscopy and SDAE-NN algorithm for predicting the cold storage time of salmon. *Journal of Spectroscopy*, 2018.

Xiong, Z., Sun, D. W., Pu, H., Xie, A., Han, Z., & Luo, M. (2015a). Non-destructive prediction of thiobarbituric acid reactive substances (TBARS) value for freshness evaluation of chicken meat using hyperspectral imaging. *Food Chemistry*, 179, 175–181.

Xiong, Z., Sun, D. W., Xie, A., Han, Z., & Wang, L. (2015b). Potential of hyperspectral imaging for rapid prediction of hydroxyproline content in chicken meat. *Food Chemistry*, 175, 417–422.

Xu, X., Xie, L., & Ying, Y. (2019). Factors influencing near infrared spectroscopy analysis of agro-products: A review. *Frontiers of Agricultural Science and Engineering*, 6(2), 105-115.

Zarei, N., & Sepyani, A. (2016). Different methods of image mapping, its advantages and disadvantages. *International Academic Journal of Science and Engineering*, 3(4), 1-10.

Zhang, H., Peng, Y., Zhao, Y., & Sun, X. (2017). Design of conveyable non-destructive detection system for meat quality. *Journal of Food Safety and Quality*, 8(8), 3192-3196.

Zhao, M., Esquerre, C., Downey, G., & O'Donnell, C. P. (2017). Process analytical technologies for fat and moisture determination in ground beef - a comparison of guided microwave spectroscopy and near infrared hyperspectral imaging. *Food Control*, 73, 1082-1094.

FIGURE CAPTIONS

Figure 1. Illustration of common modes of measurement employed with NIRs.

Figure 2. Hyperspectral systems configurations: a) One-Point, 2) Multiple spatial scanning, and c) area/plane scanning.

Figure 3. NMR spectra of a beef sample by using a HF-NMR system.

Figure 4. MRI of hams from pigs fattened with different diets (A: acorn and grass; B: high oleic acid concentrate).

Figure 1.

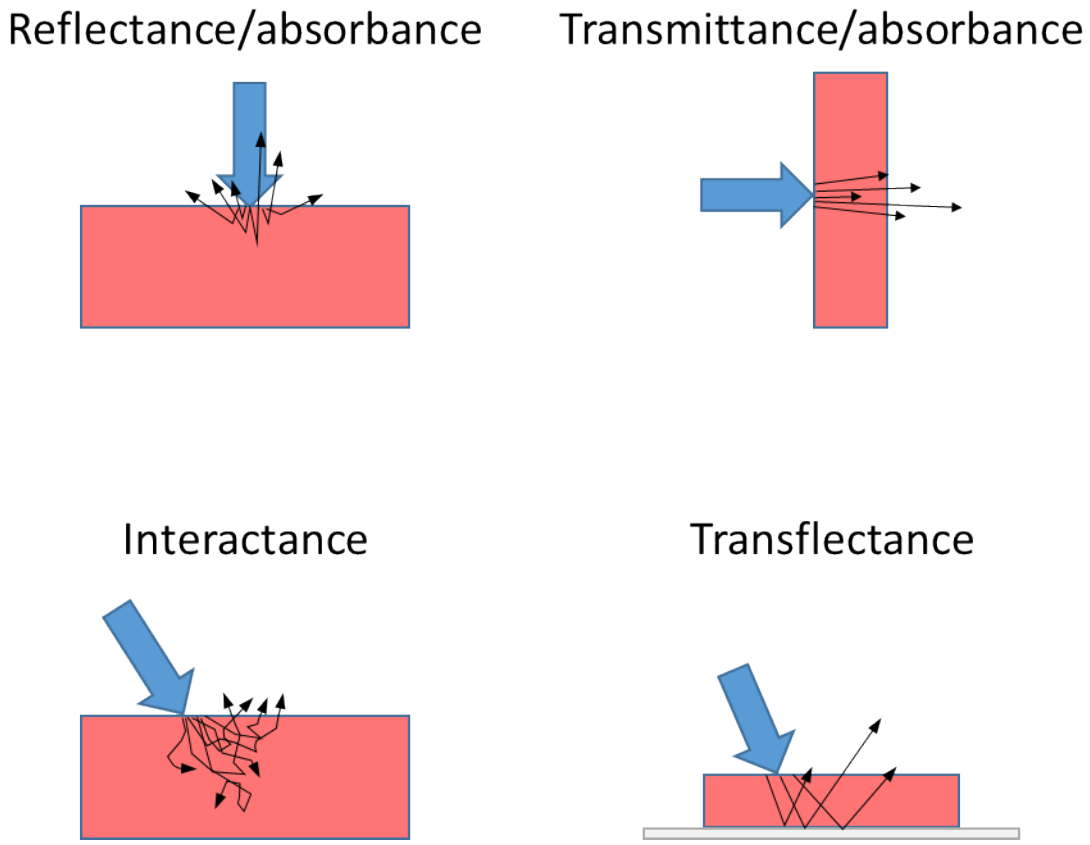
Reflectance/absorbance
Transmittance/absorbance
Interactance
Transflectance

Figure 2.

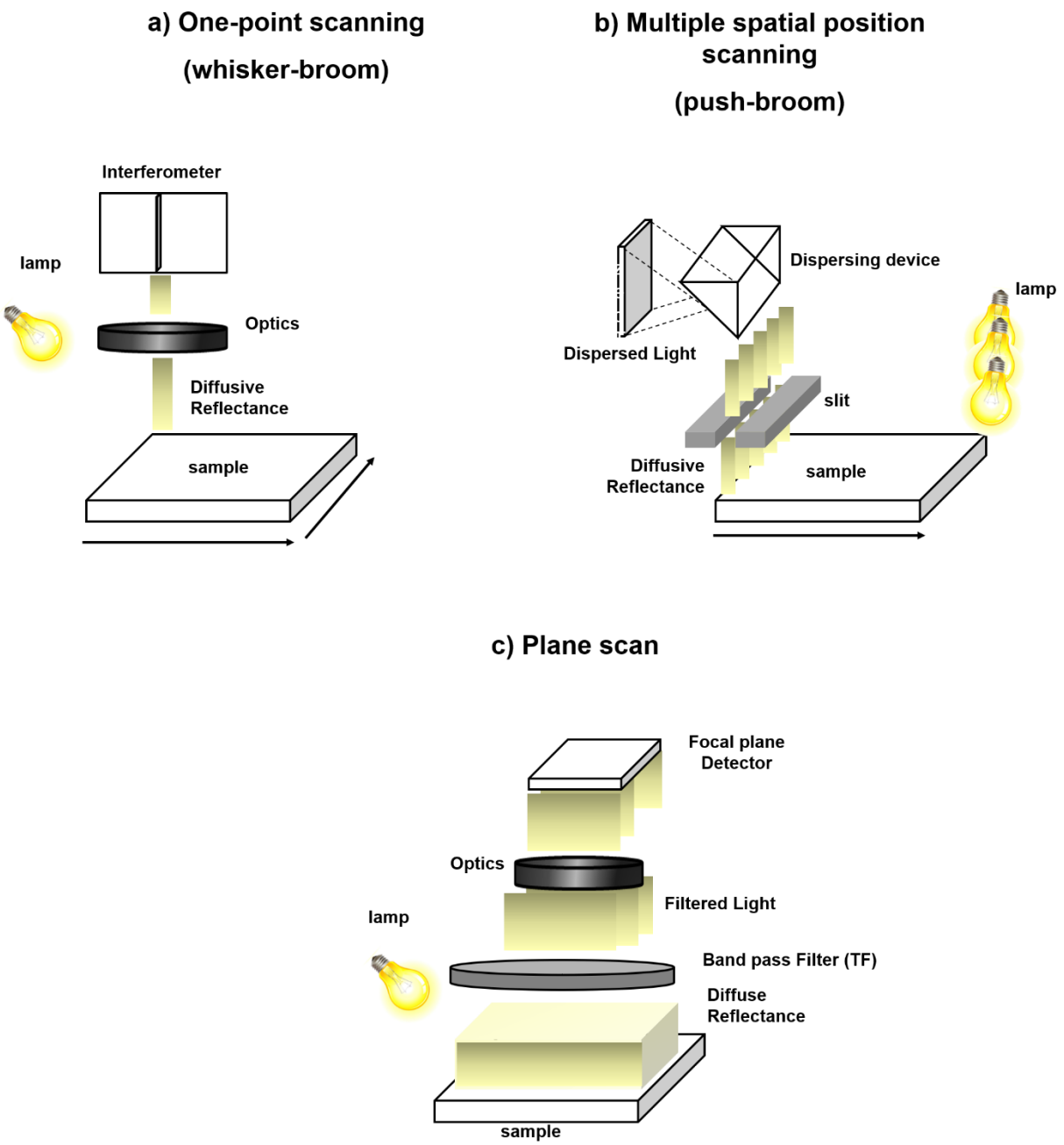
a) One-point scanning
(whisker-broom)
Interferometer
lamp
Optics
Diffusive
Reflectance
sample
b) Multiple spatial position scanning
(push-broom)
Dispersing device
lamp
Dispersed Light
slit
Diffusive
Reflectance
sample
c) Plane scan
Focal plane
Detector
Optics
Filtered Light
lamp
Band pass Filter (TF)
Diffuse
Reflectance
sample

Figure 3..

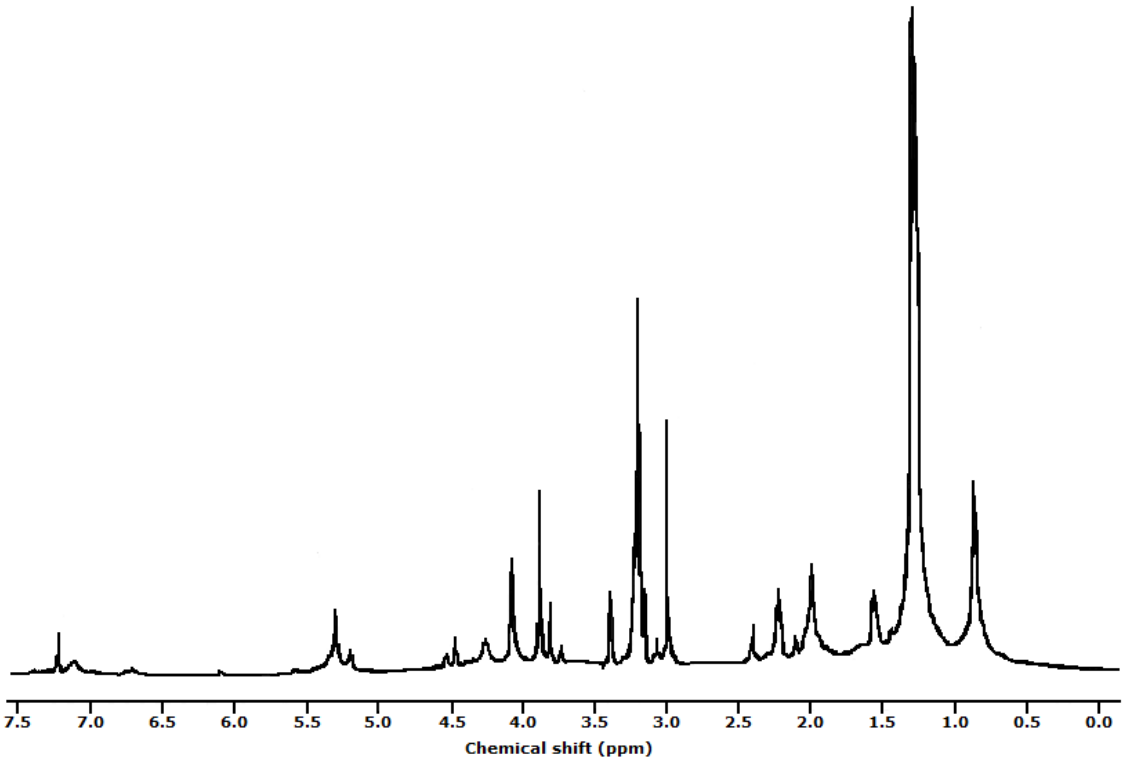

Figure 4.

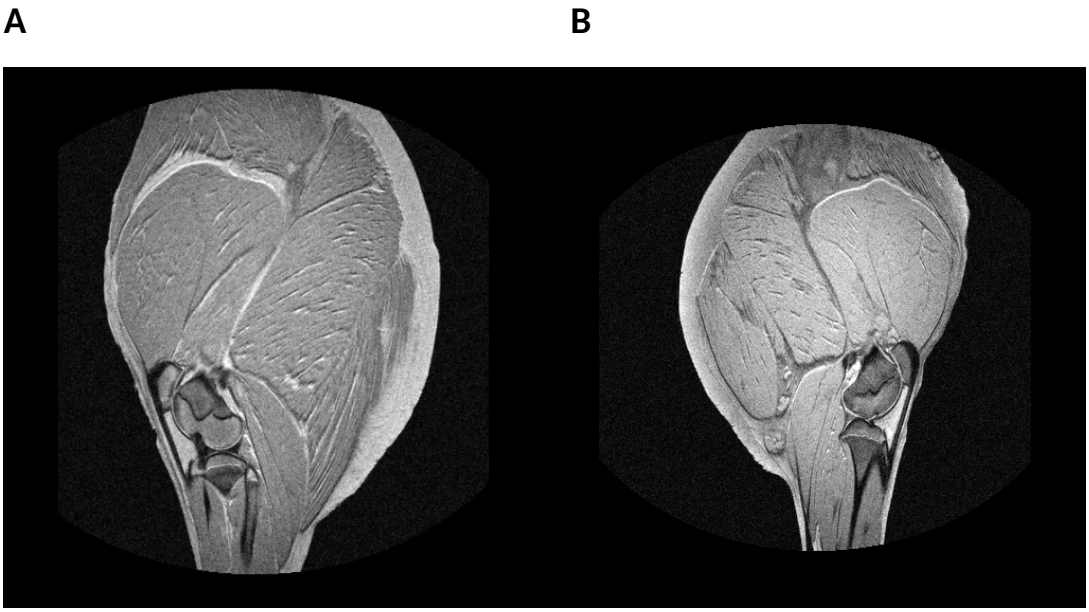

Table 1. Summary information about the use of NIRs to analyse fresh meat since 2016.

Meat sample	Sample preparation	Equipment type	Wavelength range (nm)	Data pre-processing	Data Processing	Variable	Calibration performance		Cross validation or Prediction performances		References
						Adulteration					
beef, pork, chicken	ground	benchtop	400-1700	included: none, smooth with 1st & 2nd der.[a], normalization, SNV, MSC, median center.	PLSR	Full spectrum of known species & mixes	r_c = 57-88%	RMSEC = 0.23-0.51	r_p = 53-83%	RMSEP = 0.24-1.36	Rady & Adedeji, 2018
						Selected wavelengths of known species & mixes	r_c = 90-96%	RMSEC = 0.09-0.26	r_p = 78-86%	RMSEP = 0.17-0.40	
beef, pork	ground	portable; NirScan Nano	900-1700	none, MSC, SNV, 1st or 2nd der.	PLSR	Beef	r^2_c = 0.91-0.93	RMSEC = 5.48-6.05	r^2_p = 0.33-0.70	RMSEP = 13.07-19.72	Nolasco-Perez et al., 2019
						Pork	r^2_c = 0.16-0.69	RMSEC = 11.40-18.67	r^2_p = 0.01-0.28	RMSEP = 20.32-23.90	
						Prediction					
beef	intact	portable; ASD FieldSpec	800-2500	wavelet analysis to denoise; smooth, 1st order differential, 2nd order differential, SNV.	PLS	Hardness (N)	r_c = 0.74-0.94	RMSEC = 6.25-10.19	r_p = 0.60-.079	RMSEP = 8.89-10.89	Li, Z. et al., 2016
						Springiness (mm)	r_c = 0.54-0.93	RMSEC = 0.69-1.11	r_p = 0.35-0.71	RMSEP = 0.91-1.27	
						Chewiness (mJ)	r_c = 0.69-0.94	RMSEC = 14.01-25.16	r_p = 0.52-0.66	RMSEP = 22.06-27.31	
						Adhesiveness (N·mm)	r_c = 0.44-0.72	RMSEC = 0.30-0.40	r_p = 0.22-0.69	RMSEP = 0.24-0.32	
beef	intact	benchtop; FAT-Analyzer S-7040	920-970	SG smoothing, 2nd der.	PLSR	Moisture content, over time (g/g-d·s)	-	-	r^2_p = 0.81	RMSEP = 0.34	Ishikawa et al. 2017

pork	intact	benchtop	833-2500	SG smoothing, then 1st or 2nd der. & combined with SNV or MSC; COE.	PLSR	pH	r^2_c = 69.70-78.10	RMSEC = 0.09-0.10	r^2_{cv} = 64.55-70.10	RMSECV = 0.10-0.11	Li, X. et al., 2016
						CIE L*	r^2_c = 66.31-81.90	RRMSEC = 1.72-2.32	r^2_{cv} = 60.02-11.18	RMSECV = 1.91-2.51	
						CIE a*	r^2_c = 17.26-54.55	RMSEC = 0.96-1.30	r^2_{cv} = 13.48-31.61	RMSECV = 1.16-1.32	
						CIE b*	r^2_c = 40.82-61.46	RMSEC = 0.51-0.63	r^2_{cv} = 38.38-45.49	RMSECV = 0.60-0.64	
pork	intact	benchtop; NIRFlex N-500 (Buchi)		1st der., and normalization		SFA (%)	r^2_c = 0.96	SEC=0.52	r^2_v = 0.92	SEV = 0.62	Richli et al., 2016
						MUFA (%)	r^2_c = 0.83	SEC=0.63	r^2_v = 0.76	SEV = 0.67	
						PUFA (%)	r^2_c = 0.94	SEC=0.43	r^2_v = 0.92	SEV = 0.49	
						IV	r^2_c = 0.98	SEC=0.68	r^2_v = 0.98	SEV = 0.67	
						Fat (%)	r^2_c = 0.86	SEC=1.57	r^2_v = 0.62	SEV = 1.97	
						Moisture (%)	r^2_c = 0.71	SEC=1.71	r^2_v = 0.64	SEV = 1.67	
pork	lean - homogenized; fat - intact	benchtop; FOSS NIR Systems 6500	400-2500	1100-2400nm: 1st der., SNVD	PLSR	IMF (%). Lean	r^2_c = 0.98-0.99	SEC = 0.14-0.23	r^2_{cv} = 0.95-0.97	SECV = 0.25-0.30	Prevolnik Povse et al., 2017
						Moisture (%). Lean	r^2_c = 0.90-0.91	SEC = 0.39-0.45	r^2_{cv} = 0.63-0.82	SECV = 0.65-0.75	
						Protein (%). Lean	r^2_c = 0.45-0.92	SEC = 0.48-0.92	r^2_{cv} = 0.28-0.81	SECV = 0.73-1.05	
						SFA (g/100g). Fat; Lean	r^2_c = 0.95; 0.98	SEC = 0.44; 0.26	r^2_{cv} = 0.83; 0.58	SECV = 0.79; 1.33	

						MUFA (g/100g). Fat; Lean	r^2_c = 0.98; 0.18	SEC = 0.35; 2.39	r^2_{cv} = 0.91; 0.11	SECV = 0.70; 2.54	
						PUFA (g/100g). Fat; Lean	r^2_c = 0.97; 0.78	SEC = 0.32; 1.51	r^2_{cv} = 0.89; 0.53	SECV = 0.57; 2.21	
						n-3 PUFA (g/100g). Fat; Lean	r^2_c = 0.96; 0.62	SEC = 0.04; 0.12	r^2_{cv} = 0.83; 0.55	SECV = 0.08; 0.13	
						n-6 PUFA (g/100g). Fat; Lean	r^2_c = 0.97; 0.77	SEC = 0.29; 1.43	r^2_{cv} = 0.89; 0.52	SECV = 0.51; 2.08	
						n-6/n-3 PUFA (g/100g). Fat; Lean	r^2_c = 0.80; 0.12	SEC = 0.48; 1.44	r^2_{cv} = 0.30; 0.02	SECV = 0.89; 1.52	
pork	intact	portable; Sup-NIR-1520	1000-1799	SG 1st der., SG smoothing, OSC	PLS	Cholesterol (mg/100g)	r_c = 0.91	SEC=2.56	r_p = 0.66	SEP = 4.99	Wang, H. et al., 2017
pork	Intact	benchtop; FOSS NIRSystem XDS rapid content analyzer.	400-2500	Divided into 400-1850 and 780-1850 then SNV applied to each region.	PLSR	pH (400-1850 nm)	-	-	r^2_{cv} = 0.28	RMSEV = 0.07	Andersen et al., 2018a
						EZ-Drip (%) (780-1850 nm)	-	-	r^2_{cv} = 0.06	RMSEV = 1.69	
						Vacuum drip (%) (780-1850 nm)	-	-	r^2_{cv} = 0.12	RMSEV = 1.00	
						IMF (%) (780-1850 nm)	-	-	r^2_{cv} = 0.57	RMSEV = 0.11	
pork	intact	portable; ASD LabSpec4	350-1900	One of: SG smoothing and 1st or 2nd order der., SNV, SNVD,	PLSR	Subjective firmness score	r^2_c = 0.74-0.80	RMSEC=0.41-0.48	r^2_v = 0.44-0.72	RMSEP = 0.45-0.66	Soladoye et al., 2018

				SNVD plus SG smoothing and 1st or 2nd order der.		Bar bend angle	r^2_c = 0.73-0.99	RMSEC=0.97-14.76	r^2_v=0.51-.072	RMSEP = 13.71-17.99	
lamb	homogenized	benchtop; FOSS NirSystems 6500	400-2500	Included scatter correction, der.s, smoothing	PLS, PCR	TBARS	r^2_c = 0.80-0.85	RMSEC=0.32-0.38	r^2_{cv} = 0.77-0.80	RMSECV = 0.37-0.41	Ripoll et al., 2018
lamb	intact	portable; ASD Labspec Pro	500-2000	SG 1st der.	PLS	24 h pH	r^2 = 0.37-0.70	-	-	SECV = 0.10	Knight et al., 2019
						IMF (%)	r^2 = 0.55-0.60	-	-	SECV = 0.50-0.70	
						Shear force (N)	r^2 = 0.20-0.34	-	-	SECV = 7.00-8.90	
Analysis Testing											
pork	intact	custom; in-house	350-2500	SG smoothing, SNV	PLSR, with CARS or siPLS	Moisture (%) CARS; siPLS	r_c = 0.95; 0.95	SEC = 0.58; 0.60	r_p = 0.91; 0.90	SEP = 0.38; 0.40	Wang et al., 2016
						Cook loss (%) CARS; siPLS	r_c = 0.95; 0.93	SEC = 0.01; 0.02	r_p = 0.92; 0.91	SEP = 0.02; 0.03	
						Tenderness (N) CARS; siPLS	rc = 0.94; 0.94	SEC = 3.59; 3.99	r_p = 0.90; 0.88	SEP = 6.90; 7.26	
pork	intact	portable; custom; in-house	350-2500	Included: none, SNV, SG 1st der., or combinations; model clustering	PLSR, using selected wavelengths	L*	r_c = 0.93	SEC = 0.72	r_p = 0.93	SEP = 1.16	Wang et al., 2018b
						a*	r_c = 0.97	SEC = 0.46	r_p = 0.96	SEP = 0.64	
						b*	rc = 0.97	SEC = 0.28	r_p = 0.96	SEP = 0.42	
						pH	r_c = 0.95	SEC = 0.05	r_p = 0.95	SEP = 0.06	
						TVB-N (mg/100g)	r_c = 0.97	SEC = 2.04	r_p = 0.95	SEP = 2.20	
						Fat (%)	r_c = 0.96	SEC = 0.13	r_p = 0.94	SEP = 0.18	

						Protein (%)	r_c = 0.96	SEC = 0.32	r_p = 0.96	SEP = 0.33	
						Equipment Testing					
Beef fat and lean trimmings	minced	custom; in-house; multi-point	1515-1900	SNV, SG smoothing.	PLSR	Static	r^2_c = 0.95	SEC = 5.93	r^2_p = 0.82	SEP = 3.05	Dixit et al., 2016a
						Slow motion	r^2_c = 0.9	SEC = 5.62	r^2_p = 0.92	SEP = 3.98	
						Fast motion	r^2_c = 0.95	SEC = 5.99	r^2_p = 0.85	SEP = 3.97	
fat beef trimmings & lean beef	minced	custom; in-house; multi-point	1515-2000	SNV, SG smoothing, MSC, 1st & 2nd order der., SNV plus SG smoothing.	PLSR	Fat (%)	r^2_c = 0.98-0.99	RMSEC = 2.60-4.25	r^2_p = 0.95-0.99	RMSEP = 2.79-5.67	Dixit et al., 2016b
						Moisture (%)	r^2_c = 0.98-0.99	RMSEC = 1.69-2.90	r^2_p = 0.94-0.98	RMSEP = 2.75-4.62	
						Protein (%)	r^2_c = 0.96-0.98	RMSEC = 0.96-1.36	r^2_p = 0.90-0.95	RMSEP = 1.56-2.28	
						Ash (%)	r^2_c = 0.98-0.99	RMSEC = 0.02-0.04	r^2_p = 0.95-0.99	RMSEP = 0.03-0.06	
Beef fat and lean trimmings	minced	custom; in-house; multi-point	1515-2050	SNV, SG smoothing, MSC, 1st & 2nd order der., SNV + SG smoothing	PLSR	Fat (%)	r^2_c = 0.99	SEC = 1.94	r^2_p = 0.78-0.94; baseline correction = 0.77-0.83	SEP = 6.75-8.61; baseline correction = 11.12-11.40	Dixit et al., 2016c
						Moisture (%)	r^2_c = 0.99	SEC = 1.76	r^2_p = 0.76-0.94; baseline correction = 0.74-0.84	SEP = 4.96-6.75; baseline correction = 8.49-9.22	
						Protein (%)	r^2_c = 0.99	SEC = 0.43	r^2_p = 0.85-0.91; baseline correction = 0.85-0.86	SEP = 1.71-2.27; baseline correction	

										= 2.31-2.54	
						Ash (%)	r^2_c = 0.98	SEC = 0.04	r^2_p = 0.75-0.83; baseline correction = 0.57-0.75	SEP = 0.11-0.13; baseline correction = 0.14-0.19	
pork myofibril extracts	extracted	benchtop - FOSS NIRSystem XDS rapid content analyzer	400-2500	divided into 400-700, 1100-1700, and 1700-2400, then EMSC on each.	PLSR	pH (1100-1700 nm)	-	-	r^2_{cv} = 0.14	RMSECV = 0.42	Andersen et al., 2017
pork	intact	custom; in-house	350-2500	Combinations of SG smoothing, SNV, and 1st der.		pH	r_c = 0.84-0.94	SEC=0.05-0.18	r_p = 0.79-0.91	SEP = 0.08-0.23	Wang, W. et al., 2017
						TVB-N (mg/100g)	r_c = 0.93-0.94	SEC=2.06-2.33	r_p = 0.90-0.92	SEP = 2.62-2.86	
beef	intact	in-house, portable	700-1050	2nd der., SG smoothing	PLS	MUFA	-	-	Master r^2_{cv} = 0.79; Slave r^2_p=0.69	Master SECV(%) = 1.69; Slave SEP(%) = 2.03	Piao et al., 2018
						Oleic	-	-	Master r^2_{cv} = 0.71; Slave r^2_p=0.64	Master SECV(%) = 1.86; Slave SEP(%) = 2.06	
						SFA	-	-	Master r^2_{cv} = 0.81; Slave r^2_p=0.67	Master SECV(%) = 1.67; Slave	

										SEP(%) = 2.19	
pork myofibril extracts	extracted	Benchtop - FOSS NIRSystem XDS rapid content analyzer	400-2500	Wet samples: divided into 400-900, 1100-1700, and 1700-2350 nm, then EMSC on each. Dry samples: EMSC in 1100-2500 nm only.	PLSR	Degree of proteolysis; dried	-	-	r^2_{cv} = 0.74	RMSECV = 1.42	Andersen et al., 2018b
						Degree of proteolysis; liquid	-	-	r^2_{cv} = 0.10	RMSECV = 2.61	

* **1st** or **2nd order der.:** First or second order derivative; **CARS**: Competative Adaptive Reweighted Sampling; **COE**: Constant Offset Elimination; **MSC, E-**: Multiplicative Scatter Correction, Extended-; **OSC**: Orthogonal Signal Correction; **PC1**: Principal Component 1; **PCR**: Principal Component Regression; **PLS, -R, si-**: Partial Least Squares, -regression, synergy interval-; $\mathbf{r_{c,p}}$: coefficient of correlation for -calibration, -prediction; $\mathbf{r^2_{c, cv, p, v}}$: coefficient of determination for -calibration, -cross validation, -prediction, -validation; **RMSE, -C, -CV, -P, -V**: Root Mean Square Error of -calibration, -cross validation, -prediction, -validation; **SE, -C, -CV, -P, -V**: Standard Error of -calibration, -cross validation, -prediction, -validation; **SG**: Savitzky Golay; **SNV, -D**: Standard Normal Variate, -detrend; **CIE**: Commission internationale de l'éclairage; **GC**: Gas Chromatography; **IMF**: Intramuscular fat; **IV**: Iodine Value; **MUFA**: Monounsaturated Fatty Acids; **PUFA**: Polyunsaturated Fatty Acids; **SDS-PAGE**: Sodium Dodecyl Sulfate-Polyacrylamide Gel Electrophoresis; **SFA**: Saturated Fatty Acids; **TBARS**: Thiobarbituric Acid Reactive Substances; **TPA**: Texture Profile Analysis; **TVB-N**: Total Volatile Base Nitrogen.

Table 2. Use of HSI in the analysis of fresh meat in the last decade.

Meat sample	Quality Parameter	Type od HSI	Data analysis	Model evaluation				Reference
				Calibration or Cross-validation		Prediction		
				Sample	Accuracy	Sample	Accuracy	
Chicken	Moisture	Line scan system (400–1000 nm)	PLS	52	R^2_{CV} = 0.9 SECV = 0.55 %	20	R^2_P = 0.94 SEP = 0.71 %	Kanpal et al. (2013)
	TVB-N	Line scan system (450–950 nm)	BPNN	50	R^2_c = 0.94 RMSEC= 3.95 mg/100 g	25	R_P = 0.75 RMSEP = 6.39 mg/100 g	Khulal et al. (2017)
	TBARS	Line scan system (400–1000 nm)	SPA	95	R_{cv} = 0.83 RSECV = 0.14 mg/100 g	63	R_P = 0.80 RMSEP = 0.16 mg/100 g	Xiong et al. (2015b)
Pork	Moisture	Line scan system (900–1700 nm)	PLS	80	R^2_{CV} = 0.88 SECV = 0.76 %	40	R^2_P = 0.91 SEP = 0.62 %	Barbin et al. (2013)
	IMF	Line scan system (900–1700 nm)	PLS	13	R^2_{CV}=0.94 RMSECV=0.17 %	7	R^2_P=0.97 RMSEP=0.17 %	Liu and Ngadi (2014)
	IMF	Line scan system (900 -1700 nm)	MLR	18	R_c = 0.97 RMSEC=0.89 %	6	R_P = 0.90 RMSEP = 0.92 %	Huang et al., (2017)
	TVB-N	Line scan system (400-1000 nm)	LS - SVM	48	-	24	R_P = 0.95 RMSEP = 1.86 mg/100 g	Gou et al. (2015)
	TVB-N	Line scan system (400-1000nm)	BP NN - Adaboost	48	R_C = 0.94 RMSEC = 5.30 mg/100 g	24	R_P = 0.93 RMSEP = 5.52 mg/100 g	Li et al. (2015)
	TVB-N	Fluorescence system (400–1000nm)	LS - SVM	68	R^2_C = 0.97 RMSEC 1.88 %	22	R^2_P = 0.97 RMSEP = 1.90 %	Lee et al. (2018)
	K - value	Line scan system (328–1115 nm)	PLS	140	R^2_{CV}=0.95 RMSECV=3-5	70	R^2_P = 0.92 RMSEP = 4	Cheng (2016)
	pH	Line scan system (900–1700 nm)	PLS	50	R^2_{CV}=0.87 RMSECV= 0.11	25	R^2 = 0.90 RMSEP = 0.09	Barbin et al. (2012)
	Colour (L*, a*, b*)	Line scan system (900–1700 nm)	PLS	50	L*, R^2_{CV}=0.93 RMSECV= 1.36 a*, R2CV=0.75 RMSECV= 0.67 b*, R2CV=0.89 RMSECV= 0.49	25	L*, R^2_P=0.90 RMSEP= 1.63 a*, R^2_P=0.72 RMSEP= 0.78 b*, R^2_P=0.85 RMSEP= 0.50	Barbin et al. (2012)
Beef	Moisture	Line scan system (897–1753 nm)	PLS	54	R^2_{CV}=0.89 SECV=0.51 %	27	R^2_P = 0.89 SEP = 0.46 %	Kamruzzaman et al. (2016)
	Moisture	Line scan system (880 - 1720 nm)	EMCV-PLS	36	R^2_{CV}=0.99 RMSECV=0.72 %	9	R^2_P=0.99 RMSEP = 0.64 %	M. Zhao et al. (2017)
	Fat	Line scan system (970–2500 nm)	PLS	60	R^2_{CV} = 0.89 RMSECV = 4.87 %	30	R^2_P = 0.90 RMSEP = 4.81 %	Kobayashi et al. (2010)

	Fat	Multispectral system (15 wavelength between 760 - 1040 nm)			R_{CV} = 0.98 RMSECV=3.0%		R_P=0.99 RMSEP=0.6 %	Wold et al. (2011)
	Fat	Area imaging system equipped with a filter wheel (1000–2350 nm)	PLS	126	R^2_{CV} = 0.85 RMSECV =5.85	66	R^2_P = 0.739 RMSEP =5.15	Kobayashi et al. (2012)
	Fat	Line scan system (897–1753 nm)	PLS	54	R^2_{CV} = 0.88 SECV = 0.66 %	27	R^2_P=0.84 SEP=0.65 %	ElMasry et al. (2013)
	Fat	Line scan system (400–1000 nm)	EDM	24	R^2=0.96 RMSECV = not reported	-	-	S. Lohumi et al. (2016)
	Fat	Line scan system (880 - 1720 nm)	EMCV - PLS	36	R^2_{CV} = 0.99 RMSECV = 0.79 %	9	R^2_P = 0.98 RMSEP = 0.73%	Zhao et al. (2017)
	UFAs	Area imaging system equipped with a filter wheel (1000–2350 nm)	PLS (filter based method)	126	R^2_{CV} = 0.86 RMSECV = 4.11 %	66	R^2_P = 0.64 RMSEP =3.95 %	Kobayashi et al. (2012)
	Oleic acid	Area imaging system equipped with a filter wheel (1000–2350 nm)	PLS (filter based method)	126	R^2_{CV} = 0.85 RMSECV =3.57 %	66	R^2_P = 0.71 RMSEP =3.13 %	Kobayashi et al. (2012)
	SFAs	Line scan system (970–2500 nm)	PLS	61	R^2_{CV} = 0.84 RMSECV =1.78 %	31	R^2_P = 0.87 RMSEP =1.69 %	Kobayashi et al. (2010)
	UFAs	Line scan system (970–2500 nm)	PLS	62	R^2_{CV} = 0.88 RMSECV =3.32 %	32	R^2_P = 0.89 RMSEP =3.41 %	Kobayashi et al. (2010)
	Protein	Line scan system (897–1753 nm)	PLS	54	R^2_{CV} = 0.88 SECV = 0.31 %	27	R^2_P = 0.86 SEP = 0.29 %	ElMasry et al. (2013)
	pH	Line scan system (900–1700 nm)	PLS	321	R^2_{CV} = 0.73 RMSECV = 0.06	-	-	ElMasry et al., (2012)
	Colour (L*, a*, b*)	Line scan system (900–1700 nm)	PLS	321	L*, R^2_{CV}= 0.88 RMSECV = 1.21 b*, R^2_{CV}= 0.81 RMSECV = 0.57	-	-	ElMasry et al. (2012)
	Colour (L*, a*, b*)	Line scan system (400–1100 nm)	MLR	65	L*, R^2_{CV}= 0.96 SECV = 0.61 a*, R^2_{CV}= 0.96 RMSECV = 0.75 b*, R^2_{CV}= 0.97 RMSECV = 0.19	-	-	Wu et al. (2012)
Lamb	Moisture	Line scan system (900-1700 nm)	UVE -SPA - MLR	84	R_{CV}= 0.91 RMSEC=0.56 %	42	R_P= 0.92 RMSEP = 0.58 %	Pu et al. (2014)
	Fat	Line scan system (900-1700 nm)	UVE -SPA - MLR	84	R_{CV}= 0.95 RMSECV=0.38 %	42	R_P = 0.98 RMSEP = 0.36 %	Pu et al. (2014)
	IMF	Line scan system (550 - 1700 nm)	GPR	1628	R^2_{CV} = 0.75 RMSEC = 0.43 %	829	R^2_P= 0.72 RMSEP = 0.45 %	Craig et al. (2017)

	Protein	Line scan system (900-1700 nm)	UVE -SPA - MLR	84	R_c= 0.80 RMSEC=0.36 %	42	R_P= 0.67 RMSEP 0.41 %	Pu et al. (2014)
	pH	Line scan system (900-1700 nm)	PLS	201	R_{CV}= 0.65 RMSEC=0.085	-	-	Kamruzzaman et al. (2012b)
	Colour (L*)	Line scan system (900-1700 nm)	PLS	201	R_{CV}= 0.91 RMSEC=1.32	-	-	Kamruzzaman et al. (2012b)

* **IMF**: Intramuscular fat; **SFA**: Saturated Fatty Acids; **TBARS**: Thiobarbituric Acid Reactive Substances; **TVB-N**: Total Volatile Base Nitrogen; **UFA**: Unsaturated Fatty Acids; **BP NN**: back propagation neural network; **EDM**: Euclidean distance measure; **EMCV**: ensemble Monte Carlo variable selection; **GPR**: Gaussian process regression; **MLR**: Multiple Linear Regression; **PLS**: Partial Least Squares regression; **LS – SVM**: Least Square - Support Vector Machine; **UVE-SPA-MLR**: **UVE-SPA-MLR:** Uninformative Variable Elimination - Successive Projections Algorithm - Multiple Linear Regression; $\mathbf{R_{c,CV,p}}$: coefficient of correlation for -calibration, - cross-validation, -prediction; $\mathbf{R^2_{c,cv,p}}$: coefficient of determination for -calibration, -cross-validation, -prediction; **RMSE, -C, -CV, -P:** Root Mean Square Error of -calibration, -cross-validation, -prediction; **SEP**: Standard Error of Prediction.

Table 3. Summary information about the use of NMR to analyse fresh meat in recent years.

Meat sample	Objective	Type of System	Acquisition sequences	Data analysis techniques	Main results	Reference
Pork	Relationship between cooking temperature and the water distribution within cooked pork loin.	LF	T2	PLS	High correlation coefficient on some sensory attributes (Juiciness, Tenderness)	Bertram et al., 2005
	Relationship between water holding capacity and the water distribution of cooked pork meat.	LF	T2	Correlation coefficients	High correlations as a function of different days of aging	Straadt et al., 2006
Chicken	Determining the effect of the water on frozen and thawed chicken.	LF	T2	Correlation coefficients	High correlation for water activity and cooking loss	Li et al., 2014
	Determining the water activity in chicken	LF	T2	Correlation coefficients	High correlation between water activity and T2 intensity signal.	Venturi et al., 2007
	Monitoring the cooking loss and the moisture percentage during the cooking of chicken meat.	HF	T2	ANOVA and correlation coefficients	High correlation between moisture and T2 intensity signal	Shaarani et al., 2006
Beef	Determining the moisture content of beef meat.	LF	T2	PLS and PCA	High correlation between moisture and T2 intensity signal	Pereira, and Colnago, 2012
	Discriminating between beef meat and horse meat on meat mixing.	LF	T1 and T2	PCA and Naïve-Bayes	High percentage of samples with different meat mixing were correctly classified	Jakes et al., 2015
Rabbit	Monitoring the effect of thawing and post-thawing on the quality information from frozen rabbit meat.	LF	T2	ANOVA and correlation coefficients	High correlation coefficients	Jia et al., 2017
Duck	Discriminating duck samples as function of age and its quality	HF	T1	PCA and PLS	High percentage of correct classification for duck samples.	Liu et al., 2013

* **HF**: High Field; **LF**: Low Field; **PLS**: Partial Least Square: **ANOVA**: Analysis of Variance; **PCA**: Principal Component Analysis

Table 4. Summary information about the use of MRI to analyse fresh meat in the last decade.

Meat sample	Main goals	Type of meat	Methodology				Main results	Reference
			Scanner - coil	Sequence acquisition	Image analysis	Data analysis		
Ham	Classifying as a function of pig diet	Ham	HF – H[1], body coil	SE - T1	Contour Active ROI Texture algorithms	ANOVA Pearson`s Correlation PCA	Visual differences Statistical differences in computational texture	Pérez-Palacios *et al.*, 2011b
Ham	Classifying as a function of salting stage Prediction of salt content	Ham	HF – H[1], body coil	SE - T1	Contour Active ROI Texture algorithms	Data mining (OneR, J48 decision tree MLR)	High percentages of correct classification Very good correlation coefficients of prediction	Caballero *et al.*, 2016a
Pork Loins	Optimization of the methodology Prediction of quality parameters	Pork Loins	LF - H[1], hand/wrist coil		ROI Texture algorithms	Data mining (MLR, IR)	SE – GLCM – MLR (best option for prediction)	Pérez-Palacios *et al.*, 2017
				SE - T1 GE - T1 T3D - T1	Fractals algorithms	Data mining (MLR, IR)	SE – OPFTA - MLR (best option for prediction)	Caballero *et al.*, 2017a
					Interpolation and 3D reconstruction 3D Texture algorithms	MLR and IR	GE - 3D GLCM - IR (best option for prediction)	Ávila *et al.*, 2018b
				SE - T1	A collection of 15 texture features from different algorithms	A collection of 28 regressors	Any option provides the best result for all attributes tested. All combinations achieved good to excellent correlation for most parameters analysed.	Ávila *et al.*, 2019

Pork carcass	Determining the lean meat percentage	Pork carcass	HF – H^1, large body coil	GE - T1	Interactive segmentation function for separating muscle	Stepwise regression	Accurate prediction	Bernau *et al.*, 2015
Beef	Visualization and prediction of intramuscular fat distribution	Beef	HF – H^1, head coil	SE - T1	Thresholding	Correlation coefficients	High correlation coefficients between real and predicted data	Lee *et al.*, 2015
Chicken breast	Assessment of drip after freeze/thaw	Chicken breast	HF – H^1, knee coil	3DT1 - rapid GE Proton density - turbo SE T2 - turbo SE	-	-	MRI showed freeze/thaw changes, especially when using 3DT1 - rapid GE	Frelka et al., 2019
Beef	Investigating the water distribution changes in frozen/thawed samples	Beef	LF – H^1	SE - T1 SE – T2	Signal intensity measure	-	T1 and T2 MRI displayed the decrease of water in frozen/thawed samples	Cheng *et al.*, 2019

* **HF**: High Field; **LF**: Low Field. Sequence Acquisition: **SE**: Spin Echo; **GE**: Gradient Echo; **T3D**: Turbo 3D. Image Analysis: **ROI**: Region of Interest. Data Analysis: **ANOVA**: One-Way Analysis of Variance; **PCA**: Principal Component Analysis; **MLR**: Multiple Linear Regression; **IR**: Isotonic Regression. Main Results: **GLCM**: Gray Level Co-Occurrence Matrix; **OPFTA**: One-Point Fractal Texture Algorithm.

Declaration of interests

☒ The authors declare that they have no known competing financial interests or personal relationships that could have appeared to influence the work reported in this paper.

☐The authors declare the following financial interests/personal relationships which may be considered as potential competing interests:

ANTEQUERA ROJAS MARIA TERESA - 06976064A Firmado digitalmente por ANTEQUERA ROJAS MARIA TERESA - 06976064A Nombre de reconocimiento (DN): c=ES, serialNumber=IDCES-06976064A, givenName=MARIA TERESA, sn=ANTEQUERA ROJAS, cn=ANTEQUERA ROJAS MARIA TERESA - 06976064A Fecha: 2019.12.18 09:22:01 +01'00'				PEREZ PALACIOS MARIA TRINIDAD - 76031322S Firmado digitalmente por PEREZ PALACIOS MARIA TRINIDAD - 76031322S Nombre de reconocimiento (DN): c=ES, serialNumber=IDCES-76031322S, givenName=MARIA TRINIDAD, sn=PEREZ PALACIOS, cn=PEREZ PALACIOS MARIA TRINIDAD - 76031322S Fecha: 2019.12.17 12:50:39 +01'00'
Teresa Antequera	Daniel Caballero	Silvia Grassi	Bethani Uttaro	Trinidad Perez-Palacios

AUTHOR CONTRIBUTION

Teresa Antequera: investigation and methodology in the MRI section; review; conceptualization; administration; supervision.

Daniel Caballero: investigation, methodology, writing and editing the NMR section; review.

Silvia Grassi: investigation, methodology, writing and editing the HSI section; review.

Bethany Uttaro: investigation, methodology, writing and editing the NIR section; review.

Trinidad Perez-Palacios: investigation, methodology, writing and editing the MRI section; review; conceptualization; administration; supervision.